Generation of Orbital Elements for the TELSTAR® Communications Satellites

By L. C. THOMAS

(Manuscript received December 8, 1964)

The technique now regularly in use for the generation of orbital elements for the TELSTAR communications satellites is described using angle-only and/or angle-range data versus time as input information. It is found that secular perturbation considerations are sufficient to permit trajectory prediction with pointing errors of about 0.05° over 100 orbits from a single set of elements. Modified orbital elements are chosen as the orbit description, since they explicitly express the secular rates and thereby simplify and reduce the cost of drive tape generations for the Andover ground station. The rates are derived both from perturbation theory and from direct measurement. The size and shape accuracy of the predicted orbit ellipse is improved by statistical means using trajectory data from a number of passes over a particular ground station. This permits better round-the-world predictions. Finally the computer-operator ensemble presently used for generating the orbits of the TELSTAR satellites is described.

Table of Contents

1. INTRODUCTION

The calculation of elements for orbits similar to those of recent near-earth satellites such as the first and second TELSTAR communication satellites, Echo I and II, the Tiros series and the Syncom satellites is accomplished in this analysis by considering the secular effects of the earth's gravitational potential upon the satellite's orbit. Here, the earth is taken as an oblate spheroid whose field is independent of longitude and is symmetrical about the equatorial plane. In the analysis, the gravitational effects of all bodies other than the earth are ignored, as are atmospheric drag effects and solar light pressure.[1] For orbits at distances in the thousand-mile range, luni-solar attraction can change the satellite height by no more than a few hundred feet. This can alter ground station pointing angles by less than 0.01°, which is below the resolution and tracking accuracy of the horn antenna* at Andover, Maine which supplies the bulk of the basic pointing data for Bell Telephone Laboratories use. The principal planetary perturbation is from Venus, which peaks at 3 to 4 orders of magnitude less than the luni-solar effects. Air drag effects at 1,000 miles are at least an order of magnitude below the solar gravity perturbations.

In the technique to be described, modified orbital elements (osculating elements plus explicit secular perturbations) are derived essentially from three sets of observations of the satellite. If only angle information is available, a modified form of Gauss' method is used to ascertain the range.† If some range information is available, this is added to the analy-

* This antenna has a tracking jitter of about 0.005°. Its beam can resolve the position of a satellite to within about 0.02°.

† It is recognized that the range to an orbiting celestial body cannot be ascertained if the three measured sight lines from observer to the body are coplanar.

sis. If range data for all three observations are on hand, the modified Gauss method is bypassed and elements are calculated from geometry and perturbation theory.

The degree of goodness of elements so obtained is ascertained by comparing resulting predictions of the satellite trajectory with actual data from the same pass as well as with data from passes prior to or after the one being used to generate the elements. It has been this author's experience that the fit of the predicted trajectory to the orbit from which it came is generally within 0 to 0.02°, but that the anomalistic period determination from single-pass data is not sufficiently accurate to hold the errors under 0.1° over more than a few orbits. However, this difficulty is solved by calculating two or more sets of elements from passes separated by several days and combining results to ascertain the period and other secular perturbations more exactly. Table I shows the resulting improvements under such a mode of operation for the second TELSTAR satellite.

It is to be noted that such neglected perturbations as those from the higher-order terms in the earth's potential function or solar radiation pressure may be operationally introduced by not only calculating the period from two passes separated in time, but also computing changes in the other orbital element values. This has been done in the case of Echo II to enable predictions to within 0.1° * over a time of about ten days.

The first portion of this paper presents techniques for developing orbital elements suitable for predicting future satellite pointing angles for the ground station collecting the original data. Later portions of this paper will deal with techniques aimed at producing a good round-the-world orbit fit and element rate improvement. Finally, a computer-operator ensemble used to generate modified orbital elements for the TELSTAR satellites will be described.

II. EFFECT OF DATA ON ANALYSIS

While the use of modern computers makes it entirely possible to record and process hundreds of pointing angles for each pass of a satellite,

---

In this case such a situation cannot long prevail because of the rapid motions of near-earth satellites and their orbits, as well as the rotation of the ground station on the spinning earth. Even when the orbital inclination equals the geocentric latitude of the station, only for portions of certain passes is the station in the orbit plane. The three-point orbit analysis presented here is therefore not greatly restrictive.

* This is the resolution level of the equipment which recorded the Echo II pointing angles.

TABLE I — IMPROVEMENT OBTAINED BY USING SEVERAL SETS OF ELEMENTS

Period Determined by	Initial Pass	Pointing Errors (Angular Offset)		
		10 Orbits Later	100 Orbits Later	1000 Orbits Later
Data from 1 pass	0.02	0.5°	5°	over 10°
Data from 2 passes separated by 1 day	0.02	0.03°	0.3°	1°
Data separated by 1 week	0.02	0.02	0.05°	0.3°

it is the purpose of this paper to describe techniques which can operate with a sparsity of data. The reduction of the quantity of data to be handled, even by automatic means, is of increasing importance both from a time and cost basis as more and more communications satellites and satellite systems become available. Minimizing the quantity of data is of paramount importance in implementation of small computers at tracking sites which often have very limited storage capacities, long access times, and slow machine cycles. Thus we shall be concerned with generating modified orbital elements from passes having as few as 6 or 12 data points available. Under these conditions, no statistical processing of data prior to their use in orbit generation is advisable or in many cases even sensibly possible. Rather, the procedure is to first generate elements from sets of three pointing angles (and ranges if available) on a pass, and then compare trajectories produced from these elements to the entire original set of data. By appropriate selection of triads, data points unsuitable for orbit prediction may be easily discovered and discarded, even though it may be difficult to preselect data on a purely statistical basis. For use in long-range predictions, orbital element rates (orbital period and other secular perturbations) are determined by comparisons between elements of different epochs, and these rates are used in place of the theoretical perturbations calculated in generations from a single satellite pass.

The tracking data used to determine the orbits of the TELSTAR satellites come from a single ground station. Any increase in station noise or malfunction of trajectory equipment can therefore directly affect the generated elements. Because of this, it was decided not to depend upon an uninterrupted or near uninterrupted flow of "valid" data from the ground station in any analysis but to maintain flexibility by developing elements which would predict trajectories with reasonable accuracy over a number of weeks. Concentration upon the establishment of a con-

sistent set of secular rates derived from elements generated at various epochs seemed a logical approach to this end. These rates are virtually constant for orbiting particles like TELSTAR which lose energy at an extremely low rate and whose oscillatory departures from the secular rates are not serious.

III. THE MODIFIED ORBITAL ELEMENTS

Trajectory generation is simplified by choosing a set of orbital elements in which the only perturbations are secular ones and these are explicitly expressed. This in essence reduces the trajectory prediction process to one of simple geometry. Specifically, the perturbations considered are those which produce nodal regression, perigee advance, and period modifications. They have no secular effect on the orbit inclination, eccentricity, or radius of perigee. Cyclic perturbations are ignored. A further simplication results by quoting the elements for an epoch that is the time when the satellite arrives at perigee.

No satellite moves precisely in an ellipse about the earth, and yet the elements to follow will imply plane elliptical motion. It may be helpful to consider the satellite to be moving along an ellipse in a plane which itself regresses westward due to the earth's oblateness. Superimposed upon this motion is a rotation of the major axis of the orbit ellipse about the earth's center located at one focus of the ellipse. Under these conditions, the orbital elements merely state the instantaneous position of the ellipse in space at the epoch quoted. The modified orbital elements[2] (commonly referred to as MOES) to be used in this analysis are:

Epoch — the year, month, day, hour and decimal minute at which the elements are quoted. This epoch corresponds to the time that the satellite arrives at perigee with only secular perturbations considered.

Inclination — tilt of the orbit plane in degrees referenced to the earth's equator and measured counterclockwise from the equator to the orbit plane as seen from a point above the ascending node.

West longitude of the ascending node — the west earth longitude of the ascending node of the orbit at epoch in degrees.

Prime sweep interval (PSI) — the apparent orbit regression expressed as a time. Specifically, it is the time required for a point on the earth's equator to pass under the ascending node on two successive occasions. It includes, therefore, the true regression referenced to an inertial frame, plus the apparent regression of almost one degree per day due to the earth's revolution about the sun. Often the prime sweep interval is expressed as one mean solar day (of 1440 minutes) minus M, where M is simply the number of minutes added to one day to yield the PSI.

Argument of perigee — the angle in degrees measured at the earth's center in the direction of the satellite's travel and lying between a radius vector to the ascending node position and one to perigee.

Perigee motion — the secular motion of perigee in degrees along the orbit per anomalistic period. It is positive if perigee moves in the direction of the satellite's motion.

Anomalistic period — the time in minutes required for the secularly perturbed satellite to move from perigee to the next occurring perigee. Generally, during this time the perigee is also moving.

Change in period — the change in the anomalistic period in minutes per anomalistic period.

Eccentricity— the eccentricity of the orbit ellipse. A constant under the assumed conditions of only secular perturbation and no orbit decay.

Radius of perigee — geocentric distance of the satellite at perigee in statute miles.

IV. TRAJECTORY PREDICTION

Since each TELSTAR satellite was launched, it has been a system requirement to predict the position as seen from Andover, Maine on a rather continuous basis. While the demand for predictions of the first TELSTAR satellite trajectories has decreased because that satellite is no longer active, the second TELSTAR satellite requirements have continued. Predictions currently are made for every pass of the second TELSTAR communications satellite according to the methods described herein. As a result of this type of operation it became imperative to develop a computational technique which could rapidly and economically generate trajectories on magnetic tapes capable of pointing an antenna with an accuracy of about 0.05°. The use of modified orbital elements for this purpose permitted such predictions by purely geometric means and without recourse to any integration procedures, numerical or otherwise. The method to be outlined here has been embodied into a program in regular use on an IBM 7094 computer to produce drive tapes for the TELSTAR satellites. The program execution times for a typical hour-long pass in which pointing angles are given every minute is under 0.002 hour and costs about $1 to compute. The total over-all machine cost of an hour-long drive tape is about $2, which includes the use of some auxiliary equipment.

The method of predicting pointing angles from a ground station will now be described, using the modified elements as the orbit description. The general procedure will be outlined without explicitly stating all of

the geometry, which involves mathematics no more sophisticated than spherical trigonometry.[3]

The elements specify the west longitude position of the ascending node and the argument of perigee (P) along with the secular rates so that, for each instant of time, the position of perigee is established as shown in Fig. 1.

Since the anomalistic period is given, the true anomaly V of the satellite must always be known. This, along with the orbit inclination i, describes the subsatellite latitude and longitude as functions of time. Since the radius of perigee, the eccentricity, and the satellite's true anomaly are available, the distance of the satellite above the earth's center is easily determined.

If the latitude, longitude, and height above mean sea level of the ground station are known, it becomes a matter of geometry to compute the azimuth, elevation, and slant range of the satellite from that station. Fig. 2 illustrates this. The great circle arc between *SSP* and the ground station can be computed to yield the central angle g; therefore the slant range may be found by simple triangulation, since r and R are known (see Appendix B for R calculations).

A plane tangent to a spherical earth is now inserted at the ground station. Azimuth in this plane is determined by solving the spherical

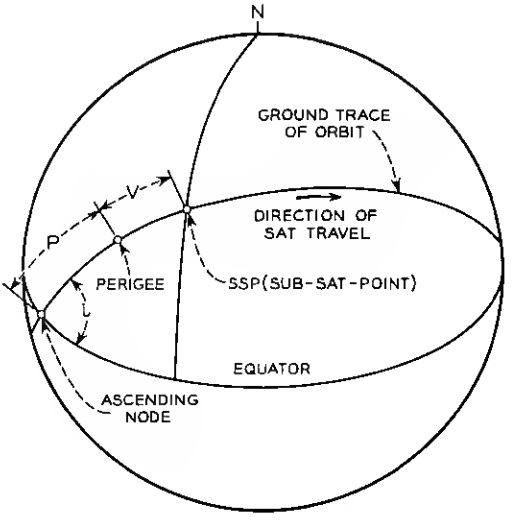

Fig. 1 — Geometry for determining the subsatellite point.

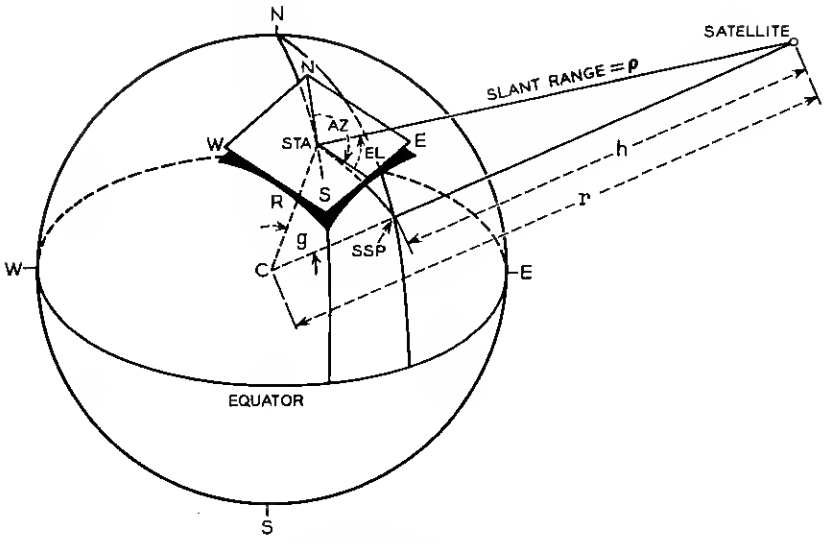

Fig. 2 — Satellite azimuth-elevation details.

triangle *N, SSP, STA* (station). Elevation is computed from the tangent plane perpendicular to *R*. Predicted azimuth and elevation referred to the oblate earth are derived from the azimuth and elevation related to a spherical earth by tipping the tangent plane north by an appropriate amount depending upon the latitude of the ground station.*

V. DETERMINING SATELLITE RANGE FROM ANGLE DATA

5.1 *A Brief History*[4]

The mathematical determination of orbits for celestial bodies began with Newton in 1680, when he calculated a parabolic orbit for a comet that appeared in that year. This was perhaps made feasible by Doerfel, who suggested that the sun lies at the focus of a cometary orbit. Euler in 1744 added to Newton's work the technique of mathematically relating time to position along a parabolic, heliocentric trajectory without prior knowledge of the orbital elements. Around 1770, Lambert added many geometrical approaches to the determination of parabolic orbits in an attempt to reduce the problem to one unknown. Shortly there-

* The amount of northward tilt of this tangent plane is equal to the difference between the geodetic and geocentric latitude of the station and is approximately $11'35.6635'' \sin 2\varphi - 1.1731'' \sin 4\varphi + 0.0026'' \sin 6\varphi$, where φ = the geodetic latitude of the station. See Ref. 5, p. 480.

after, in 1783, LaGrange added the important assumption that all observed positions of an orbiting celestial body (comet, planet, or natural satellite) lie approximately in a single plane. He also introduced a perturbation analysis to determine departures from the assumed plane. LaPlace in 1780 showed a rigorous solution[6] for an orbit formed from any conic section about the sun, using three positions of the celestial body involved as well as their first and second derivatives.* This method, though elegant, has not come into general use because of the difficulty in determining the position derivatives to sufficient accuracies.

Olbers in 1797, analytically building upon Lambert's geometry, developed a straightforward method for the calculation of paraholic orbits. The method, though not as rigorous as that of LaPlace, is sufficiently accurate and convenient to be used with little change to the present day.

To Gauss belongs the credit of developing the first coordinated approach and practical solution for the case of elliptical orbits.[7] On January 1, 1801, in searching for possible planets existing in the gap between Mars and Jupiter, the astronomer Piazzi discovered a minor planet later named Ceres. It was observed for a month before it was lost in the sun's glare. A crude projection of its motion, as well as that of the sun, indicated it would not be visible again until about October of that year. Since Ceres shines at only eighth magnitude and appears starlike through any telescope, the search for this minor planet would have been extremely difficult in those days without a good prediction of its position. Within months, Gauss developed a method for determining an elliptical orbit from a sparse bit of "angle-only" data. In his method he reduced the problem to that of two unknowns instead of one for convenience. A resulting eighth-order equation involving range and similar to that produced earlier by LaGrange was solved by Gauss by trigonometric means. The Gaussian method is essentially one of successive approximations which rapidly converge to the true range of a celestial body by appropriate iterations. With the exception of the trigonometric form of the solution that has become unnecessary in the days of high-speed digital computers, the method of Gauss has survived with little modification to the present day. The only significant computational change in the technique occurred in 1851 when Encke recast the method in Cartesian form and concerned himself with rectilinear coordinates rather than the six orbital elements of Gauss. Even now, when LaGrange's planetary equations may be numerically integrated[9,10,11] and data selected to obtain orbital elements in many chosen forms, the simple form of Gauss' solution is amenable to the addition of closed-form perturbations in an

* For a modern summary of LaPlace's method see Ref. 8, p. 168, or Ref. 9, p. 40.

iterative and rapidly converging mode of machine computation which is most conservative of time.

5.2 *General Procedure*

The adaptation of Gauss' method in the present paper will make use of the following data and assumptions:

(*i*) At least three azimuth-elevation predictions of the satellite correlated to time are available.

(*ii*) The ground station position is known (in terms of latitude, longitude, and height above mean sea level).

(*iii*) The ground station is not in the orbit plane for any of the data used.

(*iv*) The instantaneous orbit plane contains the center of mass of the earth.

The computational procedures to follow are now summarized. The first approximation of the range to the satellite is calculated using the above information, a refinement made to this first range estimate, and an initial set of orbital elements developed. Next, perturbations are calculated from the elements, the range is again refined, and so forth until no subsequent change in computed range values is observed to a chosen number of places or until this loop has been traversed a specific number of times. A final calculation of elements is then made and the resulting computed satellite trajectory compared to the measured one as a final test of the validity of the elements. Fig. 3 illustrates this procedure by a flow chart.

5.3 *Synthesizing the Range*

We begin the detailed synthesis of the range* by referring to Fig. 4, which illustrates an orbit plane about the earth along with three positions of the satellite assumed in that plane. A geocentric right-handed Cartesian coordinate system is also shown, with the z axis coinciding with the earth's spin axis, the x axis pointing toward the vernal equinox† and the y axis orthogonal to these. In this system, which does not rotate with the earth, the orbit plane may be expressed as

$$ax + by + cz = 0. \tag{1}$$

Since the three observed positions of the satellite are initially assumed to lie in this plane, each of these points must satisfy (1) and we may write

* See also Ch. 5 of Ref. 9, Ref. 12, p. 97, and Ref. 8, p. 175. For purely circular orbits see Ref. 13, p. 141.

† See p. 37 of Ref. 14.

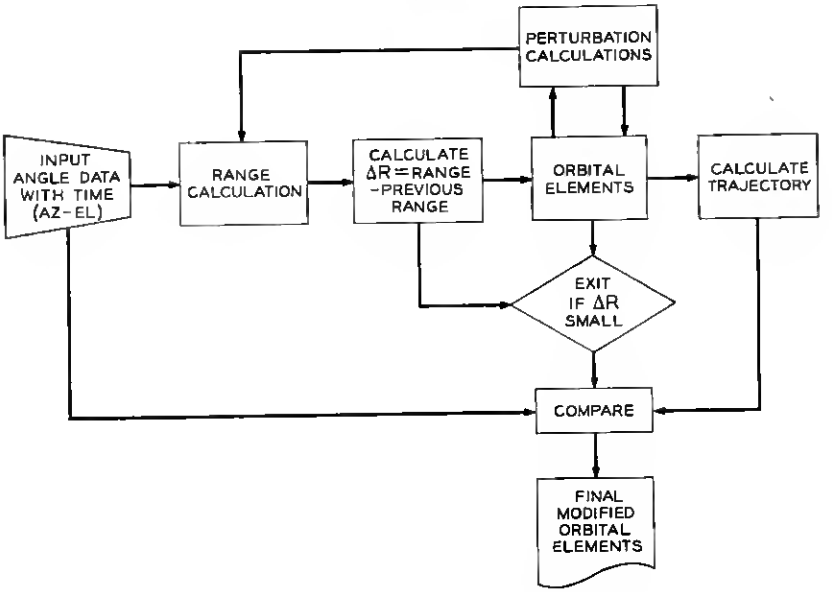

Fig. 3 — Flow chart for MOE generation.

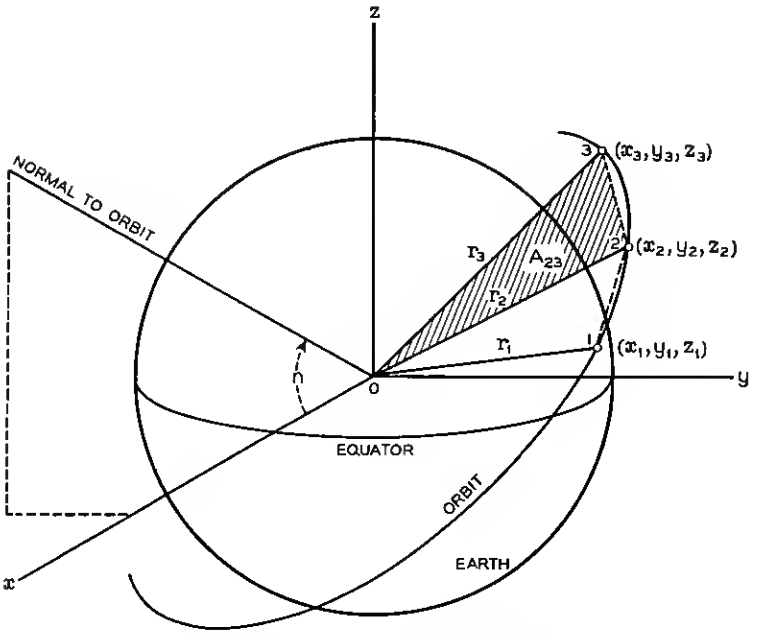

Fig. 4 — The orbit and Gaussian triangles.

$$ax_1 + by_1 + cz_1 = 0 \tag{2}$$

$$ax_2 + by_2 + cz_2 = 0 \tag{3}$$

$$ax_3 + by_3 + cz_3 = 0 \tag{4}$$

from which the determinant of the coefficients becomes

$$\Delta = \begin{vmatrix} x_1 & y_1 & z_1 \\ x_2 & y_2 & z_2 \\ x_3 & y_3 & z_3 \end{vmatrix} = 0 \tag{5}$$

permitting (2), (3), and (4) to be rewritten as

$$(y_2z_3 - z_2y_3)x_1 - (y_1z_3 - z_1y_3)x_2 + (y_1z_2 - z_1y_2)x_3 = 0 \tag{6}$$

$$(z_2x_3 - x_2z_3)y_1 - (z_1x_3 - x_1z_3)y_2 + (z_1x_2 - x_1z_2)y_3 = 0 \tag{7}$$

$$(x_2y_3 - y_2x_3)z_1 - (x_1y_3 - y_1x_3)z_2 + (x_1y_2 - y_1x_2)z_3 = 0. \tag{8}$$

In Fig. 4 twice the area (A_{23}) of the triangle 023 may be related to the coeffieient of x_1 through the angle (n) between a normal to the orbit plane and the x axis. The following equation expresses this and is derived in Appendix A:

$$y_2z_3 - z_2y_3 = A_{23} \cos n. \tag{9}$$

Similar equations may be obtained in like manner for triangles 012 and 013. When these are substituted into (6), (7) and (8) one obtains

$$A_{23}x_1 - A_{13}x_2 + A_{12}x_3 = 0 \tag{10}$$

$$A_{23}y_1 - A_{13}y_2 + A_{12}y_3 = 0 \tag{11}$$

$$A_{23}z_1 - A_{13}z_2 + A_{12}z_3 = 0. \tag{12}$$

Normalizing to A_{13}, (10), (11) and (12) become

$$m_1x_1 - x_2 + m_3x_3 = 0 \tag{13}$$

$$m_1y_1 - y_2 + m_3y_3 = 0 \tag{14}$$

$$m_1z_1 - z_2 + m_3z_3 = 0 \tag{15}$$

where

$$m_1 = A_{23}/A_{13} \tag{16}$$

and

$$m_3 = A_{12}/A_{13}. \tag{17}$$

Provided m_1 and m_3 are known, we may solve (13), (14) and (15) for

x_i, y_i and z_i ($i = 1, 2, 3$). Alternatively we may express x_i, y_i and z_i in terms of the slant ranges, ρ_i, of the satellite from the ground station and solve for these ranges in terms of m_1 and m_3. This latter route will be pursued.

Each satellite position measured from the ground station in terms of azimuth and elevation may be expressed in terms of right ascension and declination, knowing time, by standard techniques[5] (see also Appendix B). The direction cosines[15] of the line of sight from station to satellite then become

$$a_i = \cos \delta_i \cos \alpha_i \tag{18}$$

$$b_i = \cos \delta_i \sin \alpha_i \tag{19}$$

$$c_i = \sin \delta_i \tag{20}$$

where

α_i, δ_i = the topocentric right ascension and declination of the satellite.

Since the satellite is essentially orbiting the mass center of the earth, it will become advantageous to relate any topocentric coordinates of the satellite as measured from the station to the xyz geocentric ones previously specified. To do this we write

$$x_i = a_i\rho_i + X_i \tag{21}$$

$$y_i = b_i\rho_i + Y_i \tag{22}$$

$$z_i = c_i\rho_i + Z_i \tag{23}$$

where

ρ_i = the slant ranges from the station to the satellite

X_i, Y_i, Z_i = the XYZ coordinates of the station in the geocentric coordinate system of Fig. 4.

For any instant of time the X_i, Y_i, Z_i coordinates of the station may be easily derived by referring to Fig. 5. By inspection we write the direction cosines, which are quite similar to (18), (19) and (20), as

$$X_i = R \cos L \cos \alpha_i(t) \tag{24}$$

$$Y_i = R \cos L \sin \alpha_i(t) \tag{25}$$

$$Z_i = R \sin L \tag{26}$$

where

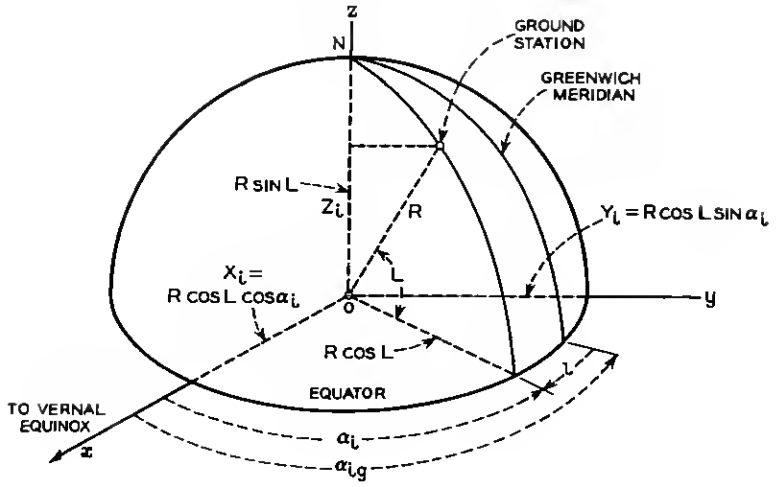

Fig. 5 — Ground station coordinates.

L = station geocentric latitude (see footnote at end of Section IV)

R = distance of station from center of the earth (see Appendix B)

$\alpha_i(t)$ = the right ascension of the station at the instant (t) of satellite observation (local sidereal time at the station).

The local sidereal time* for the above equations may be computed from

$$\alpha_i(t) = \alpha_{ig}(t) - W_1 \tag{27}$$

where

$\alpha_{ig}(t)$ = sidereal time at Greenwich in degrees†

W_1 = west longitude of the station.

A substitution of (21), (22), and (23) into (13), (14), and (15) will accomplish the desired result of expressing x_i, y_i, and z_i in terms of the slant range and topocentric position of the satellite, the station coordinates, and m_1, m_3. We obtain

$$a_1 m_1 \rho_1 - a_2 \rho_2 + a_3 m_3 \rho_3 = -m_1 X_1 + X_2 - m_3 X_3 \tag{28}$$

* See Ref. 14, p. 41.

† The term $\alpha_{ig}(t)$ may be computed from the standard meridian time for the station by standard techniques.[5]

$$b_1 m_1 \rho_1 - b_2 \rho_2 + b_3 m_3 \rho_3 = -m_1 Y_1 + Y_2 - m_3 Y_3 \tag{29}$$

$$c_1 m_1 \rho_1 - c_2 \rho_2 + c_3 m_3 \rho_3 = -m_1 Z_1 + Z_2 - m_3 Z_3 \tag{30}$$

where the unknowns are m_1, m_3 and ρ_i. A solution for ρ_2 may be obtained if $m_1\rho_1$ and $m_3\rho_3$ are eliminated from these last three equations. This yields

$$\rho_2 = D/E \tag{31}$$

where

$$D = m_1 F_1 - F_2 + m_3 F_3 \tag{32}$$

$$E = \begin{vmatrix} a_1 & a_2 & a_3 \\ b_1 & b_2 & b_3 \\ c_1 & c_2 & c_3 \end{vmatrix} \tag{33}$$

$$F_1 = \begin{vmatrix} a_1 & X_1 & a_3 \\ b_1 & Y_1 & b_3 \\ c_1 & Z_1 & c_3 \end{vmatrix} \tag{34}$$

$$F_2 = \begin{vmatrix} a_1 & X_2 & a_3 \\ b_1 & Y_2 & b_3 \\ c_1 & Z_2 & c_3 \end{vmatrix} \tag{35}$$

$$F_3 = \begin{vmatrix} a_1 & X_3 & a_3 \\ b_1 & Y_3 & b_3 \\ c_1 & Z_3 & c_3 \end{vmatrix}. \tag{36}$$

Examining (31) through (36) makes it obvious that ρ_2 is determined as soon as m_1 and m_3 are expressed by some separate consideration.

The one piece of data which has not been worked into the analysis so far is the time of flight of the satellite from point 1 to 2 to 3 (see Fig. 4). This information added to the above equations, developed solely from the geometry of the situation, will permit the solution for the range.

In Appendix C, it is shown that m_1 and m_3 are not only ratios of triangular areas formed by the radius vectors to the three satellite positions and their respective chords, but also functions of time* expressible as

$$m_1 = \frac{A_{23}}{A_{13}} = \frac{\tau_1}{\tau_2}\left[1 + \frac{\tau_3(\tau_2 + \tau_1)}{6r_2^3} + \frac{\tau_3(\tau_3^2 + \tau_1\tau_3 - \tau_1^2)}{4r_2^4}\frac{dr}{d\tau} + \cdots\right] \tag{37}$$

* Similar expressions are found in Ref. 9, p. 52, Eq. (5.3).

$$m_3 = \frac{A_{12}}{A_{13}} = \frac{\tau_3}{\tau_2}\left[1 + \frac{\tau_1(\tau_2 + \tau_3)}{6r_2^3} - \frac{\tau_1(\tau_1^2 + \tau_1\tau_3 - \tau_3^2)}{4r_2^4}\frac{dr}{d\tau} + \cdots\right] \tag{38}$$

where

$$\tau_1 = k(t_3 - t_2) \tag{39}$$
$$\tau_2 = k(t_3 - t_1) \tag{40}$$
$$\tau_3 = k(t_2 - t_1) \tag{41}*$$
$$r_2 = \text{geocentric satellite distance at time } t_2$$
$$t_i = \text{time of } i\text{th observation}$$
$$k = \text{constant for earth satellites}\dagger$$
$$= 0.07436574 \text{ min}^{-1}.$$

In (37) and (38) the geocentric range derivatives at this point are unknown, and so we approximate m_1 and m_3 by considering only the first two terms in the above equations. We shall call these estimates n_1 and n_2 respectively. Returning to (31), the range ρ_2 now may be explicitly expressed in terms of known quantities and the unknown r_2 as

$$\rho_2 \approx (1/E)[n_1F_1 - F_2 + n_3F_3] \tag{42}$$
$$\approx (1/E)[(\tau_{12} + p_{12}/r_2^3)F_1 - F_2 + (\tau_{23} + p_{23}/r_2^3)F_3] \tag{42a}$$

where

$$\tau_{12} = \tau_1/\tau_2\,, \qquad \tau_{23} = \tau_3/\tau_2 \tag{43}$$
$$p_{12} = \frac{\tau_1\tau_3(1 + \tau_{12})}{6}\,, \qquad p_{23} = \frac{\tau_1\tau_3(1 + \tau_{23})}{6}\,. \tag{44}$$

The following geometric relationship between ρ_2 and r_2 may be written by inspecting Fig. 6

$$r_2^2 = R^2 - 2R\rho_2 \cos\psi_2 + \rho_2^2 \tag{45}$$

where

$$\psi_2 = \text{the angle at the station between a line to the earth's center and one to the satellite}$$
$$= 90° + \text{elevation of satellite above a spherical earth of radius } R.$$

* Using here notation similar to Gibbs solution of Ref. 12, p. 100.

† The constant k is developed in a manner similar to the Gaussian constant for the sun, starting with the expression for the satellite period as $P = 2\pi k(a/r_e)^{\frac{3}{2}}$, where a = the semimajor axis of the orbit ellipse and r_e = the equatorial radius of the earth.

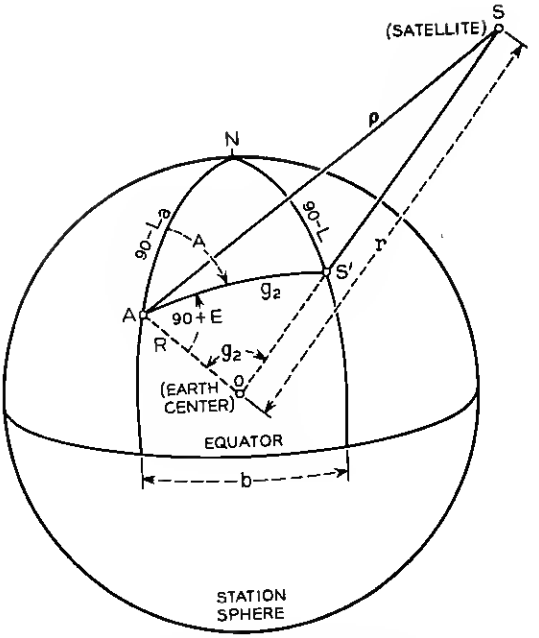

Fig. 6 — The station sphere and subsatellite points.

Equations (42) and (45) in combination permit a solution for ρ_2 and r_2. If one actually proceeds to substitute (42) into (45), an eighth-order equation similar to that derived by LaGrange results. This was later expressed by Gauss as a trigonometric, transcendental equation solved by trial-and-error methods. Rather than pursue this route, it is simpler for machine computations to assume an r_2 value (certainly greater than R_2), calculate a corresponding ρ_2 using (42), enter (45) with the r_2-ρ_2 pair, determine the departure from equality in this equation, increment the r_2 estimate, and repeat until the departure from equality is sufficiently small. By proper choice of increments, the entire procedure converges rapidly to ρ_2, r_2 values satisfying the angle-only observations, gravitational theory, and the approximate m_1, m_3 quantities used. The remaining ρ values easily follow from (28), (29) and (30).

In truncating (37) and (38) after the second term, the range derivatives were omitted in the above analysis. It is possible to return to these equations with these derivatives, which are now crudely known as first-estimate averages over the $t_3 - t_1$ interval. One could then calculate second m_1, m_3 estimates from (37) and (38), determine new r_i values, compute new geocentric range derivatives, and iterate to an r_i, ρ_i set of

solutions. This is roughly the path followed by LaGrange. By using Gauss' relationship involving certain areas of the orbit ellipse, it is possible to proceed directly to the true values of m_1 and m_3. This latter course of action, which also allows the approximations to be as close as needed, will now be followed.

In Fig. 4, we define as $\bar{y}_i$ the ratio of the areas (S_i) formed by the radius vectors r_1, r_2, r_3 and the orbit ellipse with the areas (A_i) formed by these same vectors and the chords connecting the three satellite positions. Thus the sector-triangle ratio

$$\bar{y}_1 = S_{23}/A_{23} \tag{46}$$

$$\bar{y}_2 = S_{13}/A_{13} \tag{47}$$

$$\bar{y}_3 = S_{12}/A_{12}\,. \tag{48}$$

Certainly, in terms of $\bar{y}_i$, m_1 and m_3 may be defined as [see (37) and (38)]

$$m_1 = \frac{S_{23}\bar{y}_2}{S_{13}\bar{y}_1} \tag{49}$$

$$m_3 = \frac{S_{12}\bar{y}_2}{S_{13}\bar{y}_3}\,. \tag{50}$$

If we assume pure Keplerian motion, the radius vector from the earth's center to the satellite must always sweep through equal areas in equal times.[14] This permits the direct substitution of time differences for the S factors in (49) and (50) to yield

$$m_1 = \frac{(t_3 - t_2)\bar{y}_2}{(t_3 - t_1)\bar{y}_1} = \frac{\tau_1\bar{y}_2}{\tau_2\bar{y}_1} \tag{51}$$

$$m_3 = \frac{(t_2 - t_1)\bar{y}_2}{(t_3 - t_1)\bar{y}_3} = \frac{\tau_3\bar{y}_2}{\tau_2\bar{y}_3}\,. \tag{52}$$

It is possible to determine $\bar{y}_i$ knowing the geocentric distance of the satellite and the geocentric angle through which it traveled in the measured time. This technique will be developed specifically for $\bar{y}_1$. The remaining variables $\bar{y}_2$ and $\bar{y}_3$ are derived in identical fashion. Considering then the second and third observed positions of tbe satellite, we write

$$\bar{y}_1 = S_{23}/A_{23} = \frac{k(t_3 - t_2)\sqrt{a(1 - e^2)}}{r_2 r_3 \sin 2d}\,. \tag{53}$$

The numerator of this equation expresses Keplerian motion as the radius vector sweeps area S_{23} while the denominator gives twice the area of the triangle 023. The variable d is simply the difference in the true anomalies

of the satellite at positions 2 and 3. We may shorten the notation by writing

$$\bar{y}_1 = \frac{\tau_1\sqrt{p}}{r_2 r_3 \sin 2d}. \tag{54}$$

The only unknown in this equation is p, which is a function of the size and shape of the final orbit ellipse. Since estimates of r_2 and r_3 are available at this point, p may be eliminated.[4] This permits $\bar{y}_1$ to be expressed by a cubic equation* given below:

$$\bar{y}_1^3 - \bar{y}_1^2 - a\bar{y}_1 - a/9 = 0 \tag{55}$$

where

$$a = \frac{b}{5/6 + c + \epsilon} \tag{56}$$

$$b = \frac{\tau_2}{D_y^3} \tag{57}$$

$$D_y = 2\sqrt{r_2 r_3}\cos d \tag{58}$$

$$c = \frac{r_2 + r_3 - D_y}{2D_y} \tag{59}$$

$$\epsilon = \frac{2}{35}x^2 + \frac{52}{1575}x^3 + \cdots \tag{60}$$

$$x = b/\bar{y}_1^2 - c. \tag{61}$$

It is indeed unfortunate that the factor a is ultimately a function of $\bar{y}_1$, for if this were not the case an explicit solution for $\bar{y}_1$ would exist. It turns out that ϵ is sufficiently small that it may be equated to 0 until a first estimate of $\bar{y}_1$ is found, whereupon it may then be calculated from (61) and (60) and used to derive a better estimate of $\bar{y}_1$. The estimate of $\bar{y}_1$ may be improved as much as desired by traversing this loop a multiplicity of times. Knowing the $\bar{y}_i$ values, m_1 and m_3 are next computed from (51) and (52) and entered in place of the approximate n_1 and n_3 values in (42). The three ranges to the satellite are then calculated as described earlier.

VI. GENERATING THE ORBITAL ELEMENTS

6.1 *General Procedure*

Three angular positions of a near-earth satellite as observed from a given ground station are sufficient to generate a set of orbital elements.

* See also Ref. 9, p. 56.

The addition of range data permits elements to be computed which are generally more accurate than those developed from angle only information. It will now be shown how these elements may be generated first without regard to any perturbations — as if the satellite orbited a spherical, homogeneous earth. The perturbations arising out of the earth's oblateness will then be computed, and finally their effects will be appropriately combined with the input data to produce the modified orbital elements described in Section III.

6.2 *Generating the Unperturbed Elements*

6.2.1 *Locating the Subsatellite Point.*

Given the azimuth, elevation, and range of a satellite from a specified ground station, we begin by calculating the latitude-longitude coordinates of the so-called subsatellite point. This is the point of intersection of a line, drawn from the satellite to the earth's center, with the surface of what we shall call the station sphere. This sphere is centered on the earth's center and has a radius that equals the geocentric distance of the ground station. Fig. 6 shows this. Here the central angle g_2, which lies between the station A and the subsatellite point S', is computed by solving triangle AOS. To do this, we recognize the angle OAS is known from the measured elevation of the satellite reduced to a spherical earth (see Appendix B). Thus

$$\angle OAS = 90^\circ + E \tag{62}$$

where

E = elevation in degrees of the satellite above a plane tangent to the station sphere at the station.

Since the slant range to the satellite, ρ, and the geocentric distance of the station (see Appendix B) are also known, we write

$$\cos (E + g_2) = (R/\rho) \sin g_2 \tag{63}$$

from the law of sines applied to triangle AOS. Solving for g_2 we obtain

$$g_2 = \tan^{-1}\left[\frac{\cos E}{R/\rho + \sin E}\right]. \tag{64}$$

Since g_2 must always be less than 90°, there is no angular ambiguity in this quantity as expressed above.

From the same triangle, the geocentric distance of the satellite becomes

$$r = \frac{\rho \cos E}{\sin g_2}. \tag{65}$$

The latitude and longitude coordinates of the subsatellite point are obtained by solving the spherical triangle ANS' knowing g_2 and the azimuth of the satellite, (A). By the law of cosines, the latitude of S' becomes

$$L = \sin^{-1} [\cos g_2 \sin L_a + \sin g_2 \cos L_a \cos A]. \tag{66}$$

Again, there can be no angular ambiguity since L ranges from $-90°$ to $+90°$.

The longitude of S' is determined from the longitude offset (b) of S' from A. By the law of sines

$$b = \sin^{-1} \left[\frac{\sin g_2 \cos L}{\sin A} \right]. \tag{67}$$

Angle b ranges from $-180°$ to $0°$ to $+180°$, but the direction (sign) of this longitude offset is directly determinable from the azimuth of the satellite as seen from station A. Thus the subsatellite point has been located in latitude and longitude on the station sphere.* These correspond to the geocentric latitude and longitude of S' measured on the earth.

6.2.2 *Computing Orbit Inclination and Ascending Node*

Two subsatellite points must be known for the geometrical calculation of the orbit inclination and the ascending node. Consider Fig. 7, where S_1' and S_2' represent two known positions of the subsatellite point. The orbit inclination angle i is calculated in the following manner. The great circle arc g_{12} is first computed by standard techniques, knowing the latitude and longitude of S_1' and S_2'. It is quite important, however, to remember that the earth has spun through a specific angle during the time that the subsatellite point progressed from S_1' to S_2', and both nodal regression and apsidal advance have occurred. Therefore, S_2' must be assigned a new longitude suitable to the nonrotating geometry of Fig. 7. This new longitude in degrees is

$$l_2 = l_2' - \frac{(t_2 - t_1)}{1436} 360 + N \tag{68}$$

where

l_2' = west longitude of S_2' from the Greenwich Meridian computed from the satellite azimuth, elevation, and range

* Certain special cases exist, such as when S' lies on the same meridian as A. These require no additional data and are actually simpler, since then $b = 0$, $g_2 = L - L_a$ and spherical triangle ANS' is not needed.

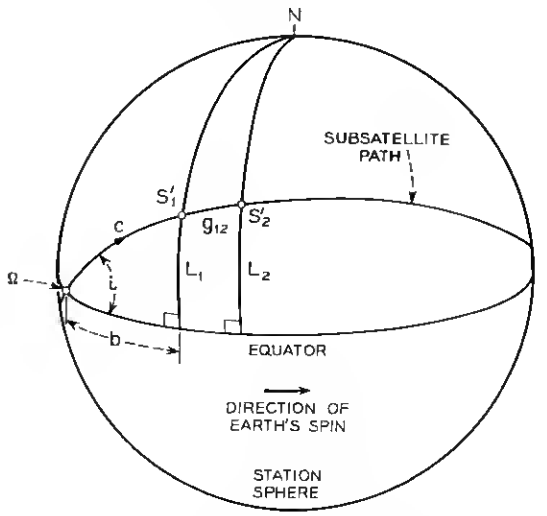

Fig. 7 — Geometry for orbit inclination and ascending node calculation.

$t_2 - t_1$ = time in minutes between the occurrence of the two measured subsatellite points

1436 = time for one earth rotation in minutes of mean solar time

N = nodal regression in time $t_2 - t_1$.*

We shall not compute the effects of apsidal advance upon the latitude and longitude of the subsatellite points, as this perturbation will be taken into account in the following section by adjusting the true anomalies.

From Fig. 7, one writes

$$\sin i = \frac{\sin L_1}{\sin c} = \frac{\sin L_2}{\sin (c + g_{12})} . \tag{69}$$

Using the last two terms of (69), one may solve for c to obtain

$$c = \tan^{-1}\left[\frac{\sin g_{12}}{\dfrac{\sin L_2}{\sin L_1} - \cos g_{12}}\right] . \tag{70}$$

Here $\sin g_{12}$ is always positive, since S_1' and S_2' correspond to satellite

* N is initially set equal to zero until an unperturbed set of elements is generated from which N may be determined: see Section VII.

positions in sight of station A. The arc c, however, may range from 0° to 180°. If the denominator of (70) is positive, c is between 0° and 90°; if negative, c is between 90° and 180°.

Knowing c, i is simply

$$i = \sin^{-1}\left[\frac{\sin L_1}{\sin c}\right] \tag{71}$$

with no ambiguity, since it ranges from 0° to 90° for proper satellites. In similar fashion, b of Fig. 7 is

$$b = \cos^{-1}\left[\frac{\cos c}{\cos L_1}\right]. \tag{71a}$$

If cos b is positive, b is between 0° and 90°; if negative, between 90° and 180°. The ascending node is then simply

$$\Omega_1 = l_1 - b \pm 360\, n \tag{71b}$$

where

l_1 = the W longitude of S_1'.
n = an integer chosen to cause Ω_1 to lie between 0° and 360°.

So far only the geometry for S_1' and S_2' both on the same side of the equator has been considered. If they are on opposite sides, then the only change is in (70), where the − sign becomes a + sign.

6.2.3 *Computing the True Anomaly along with Orbit Size and Shape.*

If the latitude and longitude positions of the three subsatellite points are known along with the corresponding geocentric satellite distances, the orbit size and shape may be computed and the satellite's true anomaly determined. To do this, consider Fig. 8, where r_1, r_2, r_3, v_{21}' and v_{31}' are all known. The values for r_1, r_2, r_3 were obtained by (65), and v_{21}, v_{31} are merely the great circle arcs between S_2' and S_1' and between S_3' and S_1', respectively, corrected for earth spin and later for regression per (68). It is assumed that perigee moves in a secular manner along the orbit ellipse during the time of travel of the satellite from 1 to 2 to 3. Consequently the true anomaly differences determined geometrically must be corrected as follows

$$v_{21}' = v_{21} + \frac{\Delta P(M_2 - M_1)}{2\pi} \tag{72}$$

$$v_{31}' = v_{31} + \frac{\Delta P(M_3 - M_1)}{2\pi} \tag{72a}$$

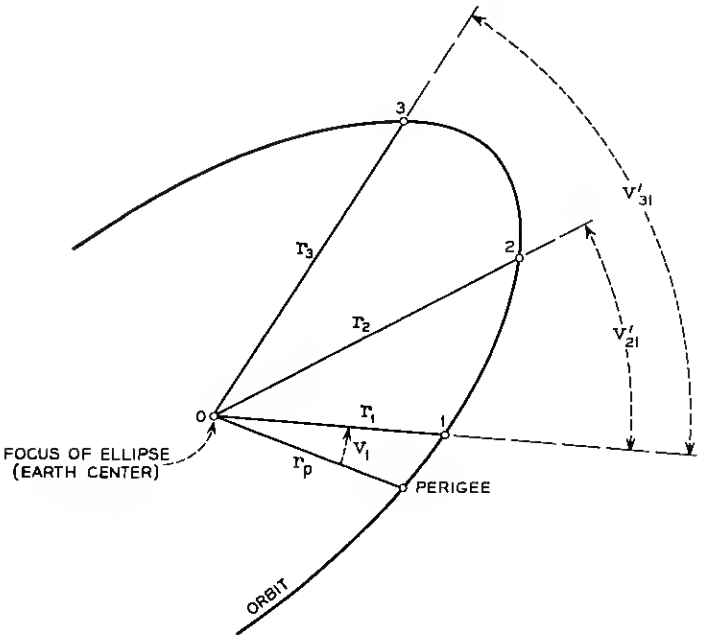

Fig. 8 — True anomaly geometry.

where

v_{21} , v_{23} = the geometric true anomaly differences
ΔP = the apsidal advance in degrees per anomalistic period
M_1 , M_2 , M_3 = the mean anomalies* of the satellite at 1, 2, and 3 respectively.

Quite clearly the mean anomalies are not known until the position of perigee is determined. Thus, the corrections of (72) and (72a) are not applied to v_{21} and v_{31} until first estimates of the perigee position and of the apsidal advance rate are obtained. At that time a first estimate of the true anomalies of the satellite is known, and this is used to determine a first estimate of the mean anomalies. With these values, (72) and (72a) are used to correct the purely geometrical true anomalies and the loop is traversed until no further significant changes in v_{21}' or v_{31}' are observed.

Let us now set

* See Ref. 9, p. 113.

$$p = a(1 - e^2) \tag{73}$$

where

a = the semimajor axis of the orbit ellipse
e = eccentricity of the orbit ellipse.

Then for the three satellite positions the polar form of the ellipse* becomes

$$r_1 = \frac{p}{1 + e \cos v_1} \tag{74}$$

$$r_2 = \frac{p}{1 + e \cos (v_1 + v_{21})} \tag{75}$$

$$r_3 = \frac{p}{1 + e \cos (v_1 + v_{31})} \tag{76}$$

where

v_1 = the true anomaly of the satellite at position 1.

It is helpful to rewrite these three equations as

$$e \cos v_1 = (p/r_1) - 1 \tag{77}$$

$$1 + Ae \cos v_1 + Be \sin v_1 = p/r_2 \tag{78}$$

$$1 + Ce \cos v_1 + De \sin v_1 = p/r_3 \tag{79}$$

where A, B, C and D are all known quantities defined as

$$A = \cos v_{21} \tag{80}$$

$$B = -\sin v_{21} \tag{81}$$

$$C = \cos v_{31} \tag{82}$$

$$D = -\sin v_{31}\,. \tag{83}$$

Solving for p in (77), (78) and (79) yields

$$p = \frac{C - 1 + D(1 - A)/B}{\frac{C}{r_1} - \frac{1}{r_3} + \frac{D}{B}\left(\frac{1}{r_2} - \frac{A}{r_1}\right)}. \tag{84}$$

All quantities in the right-hand member of this equation are known, so that p is determined. Returning to (77) and (78), the solution for the true anomaly is

* See Ref. 9, p. 116.

$$v_1 = \tan^{-1}\left[\frac{\sin v_1}{\cos v_1}\right] = \tan^{-1}\left[\frac{\frac{1}{B}\left\{\frac{p}{r_2} - 1 - A\left(\frac{p}{r_2} - 1\right)\right\}}{\frac{p}{r_1} - 1}\right] \quad (85)$$

unless $(p/r_1) - 1$ is zero, which occurs for a circular orbit. In this case, the solution for v_1 is of little importance and may be arbitrarily set to 90°.

In general, the true anomaly ranges from 0 to 360°, but all quadrant ambiguities in (85) may be resolved by observing the algebraic sign of sin v_1 and cos v_1, expressed by the numerator and denominator of the final fraction in (85).

With v_1 known, the eccentricity from (77) is simply

$$e = \frac{\frac{p}{r_1} - 1}{\cos v_1}. \quad (86)$$

The radius of perigee from (73) is

$$r_p = p\left(\frac{1 - e}{1 - e^2}\right). \quad (87)$$

6.2.4 *Reduction to Epoch*

One of the features of the modified orbital elements is that they are quoted for the epoch at which the satellite passes through perigee. The node and perigee positions as well as the true anomaly of the satellite determined in the preceding sections were computed for the time of the first data point. They must now be reduced to the time of perigee passage.

During the time the satellite moved from perigee to the first data point, the earth rotated, the orbit node regressed, and the perigee moved. The angular velocity of the earth is known and the node and perigee motions are secular functions of i, e, and r_p, as will be shown later in Section VII. Consequently it is possible by calculation to "move the satellite" back to perigee, taking into account these other motions as well. To do this we shall assume Keplerian motion along an ellipse whose perigee moves in time. If we knew the true anomaly of the satellite at position 1, refereneed to the moving perigee, we could determine the time required for the satellite to orbit from perigee to data point number 1. This true anomaly may be obtained in an iterative manner using

$$v_1' = v_1 + \Delta P(M_1/2\pi) \quad (88)$$

where

ΔP = apsidal advance in degrees per anomalistic period
M_1 = the mean anomaly of the satellite at data point 1
v_1 = the geometrical true anomaly of satellite when at point 1 (from Section 6.2.3).

A first estimate of M_1 is obtained from v_1 using Kepler's equation. This permits a first estimate of v_1' by using (88), which in turn allows a second estimate of M_1 based on the first v_1' estimate. The procedure cycles until further changes in v_1' are insignificant. The final value of M_1 corresponding to the final v_1' is used to determine the time of flight of the satellite from perigee to the first data point, which is

$$t_b = (M_1/2\pi)T_a \tag{89}$$

where

T_a = the anomalistic period in minutes.

The elements are back dated by the amount t_b to produce modified orbital elements. In these the ascending node is simply

$$\Omega = \Omega_1 + \Delta\Omega t_b \tag{90}$$

where

Ω_1 = the west longitude of the node at data point no. 1
$\Delta\Omega$ = the regressional rate in degrees per minute.

Similarly, the argument of perigee is

$$P = P_1 + \Delta P(M_1/2\pi) \tag{91}$$

where

P_1 = the perigee position at data point no. 1
ΔP = the apsidal advance rate in degrees per anomalistic period.

6.2.5 *The Anomalistic Period*

The anomalistic period may be computed from the mean anomalies at the data points (after these are known from the first estimate of the orbital elements) and the times of flight through these points. For example, one may write

$$T_a = \frac{2\pi(t_2 - t_1)}{M_2 - M_1} \tag{92}$$

or

$$T_a = \frac{2\pi(t_3 - t_1)}{M_3 - M_1} \tag{93}$$

or

$$T_a = \frac{2\pi(t_3 - t_2)}{M_3 - M_2} . \tag{94}$$

Equally well, T_a may be computed from the finally determined values of i, e, and r_p by methods outlined in Section VII.

6.3 *Adding the Perturbations to the Orbital Elements*

In the derivation of the modified orbital elements, perturbations seem required before sufficient orbital data are available for their computation. The general technique is to assume all perturbations zero until a first set of elements has been calculated for epoch t_1, then to supply these perturbations to produce a second set of elements, and to continue this iteration until further element changes are insignificant. Thus the N of (68), the ΔP of (72), (72a), and (88), and the T_a of (89) follow this route.

For orbits of the TELSTAR satellites which have had eccentricities of up to 0.4 and r_p values as low as 4556 statute miles, convergence by the above method occurs within three iterations. Four iterations are normally required for eccentricities up to about 0.8.

VII. THE SECULAR PERTURBATIONS

7.1 *Perturbation Theory and Formulae*

The perturbations to be outlined here are secular and produced only by the earth's oblateness. The gravitational field therefore will be independent of the longitude and symmetrical about the earth's equator. Its potential* may be expressed as

$$U = \frac{GM}{r}\left[1 - \sum_{n=1}^{\infty} J_n \left(\frac{R_E}{r}\right)^n P_n(\cos L_c)\right] \tag{95}$$

where

J_n = constants determined in the first instance by observation of many satellites

* See Ref. 16, p. 4.

R_E = the equatorial radius of the earth = 3963.347 statute mi.
r = the geocentric satellite distance
$P_n(\cos L_c)$ = the Legendre polynomial of order n
L_c = the geocentric colatitude of the satellite.

Writing (95) using only the J_2 terms, we have

$$U = \frac{GM}{r}\left[1 + \frac{1}{2}J_2\left(\frac{R_E}{r}\right)^2(1 - 3\cos^2 L_c)\right] \qquad (96)^*$$

where

GM = Newton's universal gravitational constant times the mass of the earth[16,17]
= $(3.44280 \pm 0.000026) \times 10^8$ statute miles^3/minutes^2
J_2 = $\frac{2}{3}$ × Jeffreys' J (see Refs. 18 and 19)
= 1.0827×10^{-3}.

Equations of motion for a satellite orbiting this oblate earth are found by setting the spherical polar components of acceleration equal to

$$\frac{\partial U}{\partial r}, \quad \frac{1}{r}\frac{\partial U}{\partial L_c}, \quad \text{and} \quad \frac{1}{r\sin L_c}\frac{\partial U}{\partial \varphi},$$

where r, L_c, and φ are the spherical coordinates of the satellite. After a bit of work, the following secular rates of the orbital elements are produced. For the secular nodal regression† in radians per nodal period we have

$$\begin{aligned}\Delta\Omega &= -3\pi J_2\left(\frac{R_E}{p}\right)^2\cos i + OJ^2 \\ &= -0.16028\frac{\cos i}{p^2}10^6\end{aligned} \qquad (97)$$

where

* $J_1 = 0$ since the orbit plane is assumed to include the center of mass of the earth.

† Many authors have derived perturbation equations for orbital elements and expressed them in numerous ways, quite often with great elegance and detail. It may seem, therefore, that (97) is unduly simple. This analysis, however, is confined to secular rates only. It can be shown that contributions to these rates from the third through the sixth zonal harmonics of the earth's potential function (as well as from the J_2^2 terms) are about three orders of magnitude less than the J_2 contribution given by (97). They are, therefore, omitted in this analysis where long-term predictions of pointing angles need only be accurate to within 0.05°. Secular contributions to the orbit eccentricity and inclination are also of order J_2^2 and omitted. (See Ref. 21 for expressions of higher-order terms.)

$$p = a(1 - e^2)$$
$$OJ^2 = \text{terms of tbe order of } J^2 \text{ which are omitted.}$$

The secular apsidal advance rate becomes

$$\Delta\omega = -\frac{3}{2}\pi J_2 \left(\frac{R_E}{p}\right)^2 [1 - 5\cos^2 i + Oe^2]$$
$$= 0.08014 \frac{(5\cos^2 i - 1)}{p^2} 10^6 \tag{98}$$

in radians per nodal period. Finally, the nodal period which expresses the energy in the ellipse is

$$T_n = \frac{2\pi\left(\frac{a^3}{GM}\right)^{\frac{1}{2}}\left[1 - \frac{3}{4}J_2\left(\frac{R_E}{p}\right)^2 (5\cos^2 i - 1)(1 - e^2)^{\frac{1}{2}}\right]}{1 + \frac{3}{2}J_2 \frac{R_E{}^2}{a^2(1 - e^2)^3}} \tag{99}$$

where

$$2\pi/(GM)^{\frac{1}{2}} = 3.38629354 \times 10^{-4} \text{ minute/statute miles}^{3/2}.$$

The prime sweep interval of the modified orbital elements is related to the true nodal regression by the following expressions

$$\Delta\Omega' = \frac{\Delta\Omega \times 82505.92}{T_n} \quad \text{deg/day} \tag{99a}$$

$$\text{PSI} = 1440 - \frac{4(\Delta\Omega' + 0.9856)}{1 + \frac{\Delta\Omega' + 0.9856}{360}} \quad \text{minutes.} \tag{99b}$$

The rates for the modified orbital elements are not complete until the anomalistic period has been derived. This may be accomplished knowing T_n and $\Delta\omega$. The procedure is outlined below.

7.2 *Determining the Anomalistic Period from the Nodal Period*

We bave defined the anomalistic period as the time required for the satellite to move from perigee to the next perigee. The two perigee positions are shown as points p_1 and p_2 in Fig. 9, where it is seen that the angular motion of the satellite in the time T_a may exceed 360°. During this time the perigee itself is in motion and its rate is expressed by (98).

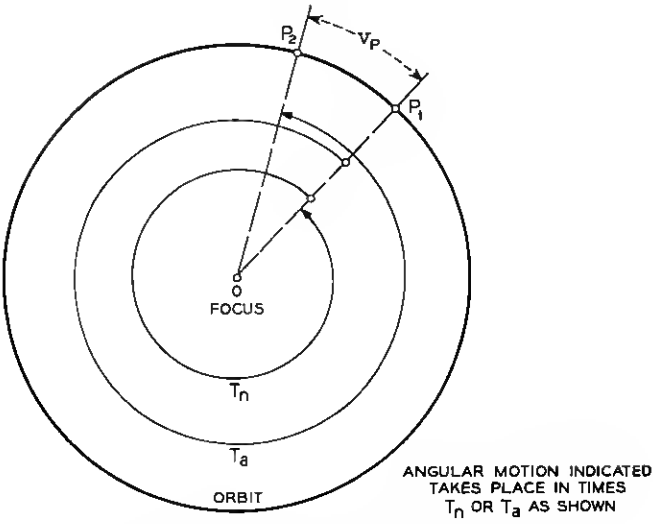

Fig. 9 — Relationship between T_n and T_a.

Thus the anomalistic period exceeds* the nodal period by an amount t so that

$$T_a = T_n + t \tag{100}$$

or

$$T_a = (1 + f)T_n \tag{101}$$

$$= \left(1 + \frac{M}{2\pi}\right) T_n \tag{102}$$

where

t = the time for the satellite to move from p_1 to p_2
f = the fraction of T_n represented by t
M = the mean anomaly corresponding to f.

We may also express the motion of perigee in time T_a as the angle

$$v_p = \Delta\omega \; T_n/T_a \,. \tag{103}$$

If T_a is initially set equal to T_n, then (103) represents a first estimate of v_p from which a first estimate of f may be computed from

* If $\Delta\omega$ is negative, T_n exceeds T_a, but the conversion equations are still valid.

$$E = 2 \tan^{-1}\left[\left(\frac{1-e}{1+e}\right)^{\frac{1}{2}} \tan \frac{v_p}{2}\right] \tag{104}$$

and

$$M = E - e \sin E. \tag{105}$$

By (102) a first anomalistic period estimate is obtained which can yield a second estimate of v_p by (103), and the process is iterated until successive changes in T_a are sufficiently small. Since (102) through (105) contain essentially two unknowns, v_p and T_a, closed-form approximate solutions are possible by using truncated series of expansions of the tangent and sine functions. The iterative method, however, has the advantage that the accuracy is limited only by the number of times that the user is willing to traverse the loop.

Knowing the anomalistic period, it is straightforward to express the nodal regression and apsidal advance in degrees per anomalistic period suitable for use in the modified orbital elements.

VIII. ROUND-THE-WORLD ORBIT PREDICTIONS

So far, techniques have been presented for developing orbital elements suitable for predicting future satellite pointing angles. These predictions suffer little error when referred to the ground station which took the original data. However, if predictions are made for other stations, the errors can be greater due simply to the fact that the elements were derived from only a small portion of the orbit ellipse — a fact which makes it difficult to assess the size and shape of the ellipse. The effect will be most pronounced if the latitude of the second station differs greatly from that of the first* as, for example, the case of elements generated from Andover, Maine, trajectories and used for Woomera, Australia, predictions. In previous works this problem is simply solved by obtaining data from stations spaced around the world and using it in orbit generation. In this paper it is desired to confine the data taken to one station and yet predict for remote stations located anywhere. This is accomplished by recognizing that, during the course of a day, a single base station sees a good portion of the orbital ellipse on successive passes. For each such pass a set of elements may be generated. Each set will about equally well describe the orbit over the base station, but can diverge in predictions for stations at different latitudes as illustrated by

* It should be recognized that stations at different longitudes (but at equal latitudes) are not to be considered unique, since they essentially observe the same portions of the orbit at different times of day.

exaggeration in Fig. 10. This is due principally to estimating the size and shape of the orbit ellipse from data which necessarily contain some measurement error. One could improve the situation at remote stations by placing an ellipse of best fit through all the essentially different base station trajectories and thereby gain a better estimate of the eccentricity and radius of perigee in the orbit. If base station predictions made from elements that fit each individual pass are excellent, one could equally well fit an ellipse by a least-squares method to the predicted rather than the measured base station data, and still improve the situation at remote stations. As a matter of fact, proceeding from good base station predictions tends to smooth the input data by bringing them into accord with the motions permitted by gravitational theory and this, in a sense, filters some of the observation noise.

The technique for this round-the-world fit proceeds in detail as follows. Modified orbital elements are used to predict the true anomaly and the

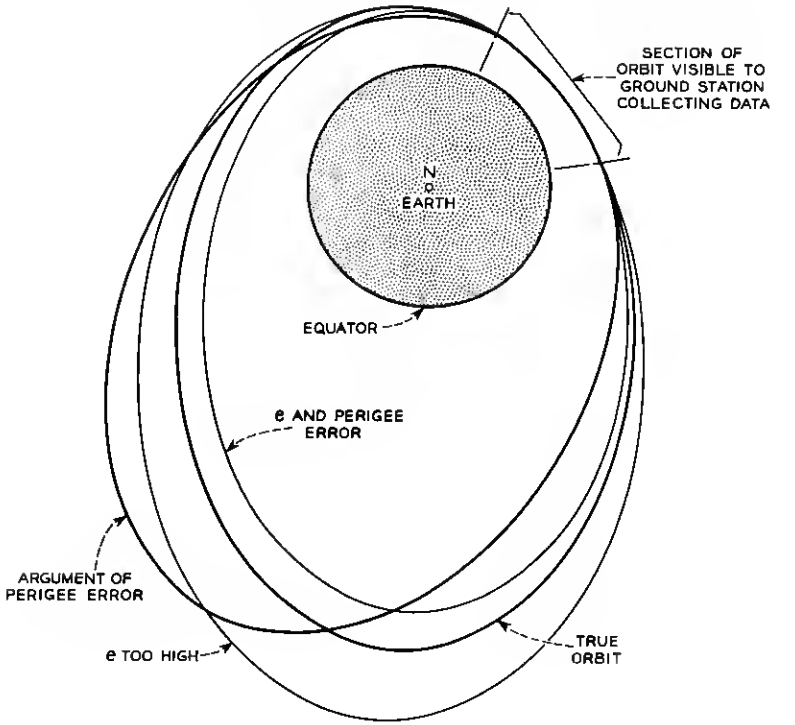

Fig. 10 — Projections of orbits on equatorial plane.

corresponding geocentric distance of the satellite for a set of passes seen from the base station. The polar equation of the ellipse is then written as follows:

$$\frac{1}{r} = \frac{1}{a(1 - e^2)} + \frac{e \cos v}{a(1 - e^2)} \tag{106}$$

$$= B_0 + B_1 \cos v. \tag{107}$$

The predicted true anomaly-geocentric distance pairs are then used to determine B_0 and B_1 of (107) by standard least-squares methods. It is important to note that the true anomaly v of (107) must always be referred to the moving orbit perigee as was done in Section 6.3.

Providing that e and r_p do not seriously change their magnitude during the set of passes being considered (that is, no great orbit energy loss), we may determine these quantities from the least-squares B_0 and B_1 values to be

$$e = B_1/B_0 \tag{108}$$

$$r_p = \frac{1 - e}{B_0(1 - e^2)}. \tag{109}$$

While the determination of orbit size and shape for round-the-world orbit predictions may be carried out by least-squares methods, the node position and argument of perigee are often treated differently, since they are not determined to the same degree of accuracy by each pass of the satellite over the base station. Pass selection is often a good procedure to follow for these parameters. For example, data from a pass that contains perigee are generally considered much more likely to produce a more nearly accurate measure of the perigee argument than those from a pass which does not. The same is true of the ascending node.

IX. IMPROVING THE ELEMENT RATES BY DIRECT MEASURE

Quite obviously, if the modified orbital elements are known at two separate epochs, the secular rates may be computed directly. Let us assume that the elements are correct except for the rates of nodal regression, anomalistic period, and apsidal advance.

9.1 *Nodal Regression*

The west longitude of the ascending node at the earlier epoch (Ω_1) is related to its position at the later epoch (Ω_2) by

$$\Omega_2 + 360\Delta - \Omega_1 = \frac{360 t_{12}}{\text{PSI}} \text{ degrees} \tag{110}$$

where

t_{12} = time interval in minutes between the two epochs
PSI = the nodal regression expressed as the prime sweep interval ($1440 - M$ minutes)
A = an integer which may have any positive, negative or zero value.

Examination of (110) reveals ambiguities in multiples of 360° in the determination of the prime sweep interval, since without some knowledge of its magnitude, one cannot be sure if the node has regressed more than one revolution to its Ω_2 position. The theoretical value of the prime sweep interval is available, however, by the techniques of Section VII. Thus the ambiguity is avoided unless t_2 is extremely large, which allows even small variations in PSI to promote as much as one revolution difference in nodal regression. Solving (110) for the prime sweep interval, we have

$$\text{PSI} = \frac{360 t_{12}}{\Omega_2 - \Omega_1 + 360A} \text{ minutes.} \tag{111}$$

9.2 *Anomalistic Period*

From the epochs of the two sets of modified orbital elements on hand, a single anomalistic period, having zero rate of change, may be computed. First, the whole number of satellite passages through perigee in the time t_{12} between epochs is expressed as

$$A_n = \text{INTF}\ (t_{12}/T_{at}). \tag{112}$$

Then a refined estimate of the anomalistic period becomes

$$T_a = t_{12}/A_n \tag{113}$$

where

T_{at} = theoretical anomalistic period computed from the first set of MOES using (99) through (105)
INTF = indicates that only the integer portion of the division is to be retained.

Sometimes the anomalistic period of a particular set of elements has been well refined by the above procedure, so that it is quite precise over a short period of time. If, some time later, a second set of elements is determined and shown to fit the orbit well at this later time, then it is often a good procedure to retain the initial anomalistic period and compute a period change to be consistent with the satellite's arrival at perigee

on epoch 2. This incidentally, is the ouly manner in which a change in period is deduced for the TELSTAR satellites. The procedure is as follows. Calculate A_n using (112) as before. A first estimate of the change in period per period becomes

$$\Delta T_a = \frac{2t_{12} - A_n T_{at}}{A_n^2}. \tag{114}$$

It is possible that the A_n value calculated by (112) is not eorrect owing to the change in the period during the interval t_{12}. Therefore we compute a time interval t_f as a trial to compare to t_{12}

$$t_f = A_n T_{at} + (A_n^2/2)\Delta T_a \tag{115}$$

and if t_f exceeds t_{12}, we decrease A_n by 1 and repeat the operations of (114) and (115) iu an iterative sensc until t_f is less than t_{12}. (Of eoursc, if t_f ever equals t_{12} in the process, then the corresponding A_n value is eorrcct and no further iteration is needed.) When t_f is less than t_{12} compute

$$t_{f1} = (A_n + 1)T_{at} + \tfrac{1}{2}(A_n + 1)^2 \Delta T_a \tag{116}$$

and if t_{f1} exceeds t_{12}, thc current A_n value is valid. If t_{f1} is equal to t_{12} then A_n should be dcrcased by one. If t_{f1} is less than t_{12}, increase A_n by onc and repeat the process from (114) on. Eventually the procedure converges on an A_n value that either makes t_f equal to or less than t_{12} and t_{f1} greater than t_{12}. The corresponding ΔT_a is the proper one to use.

9.3 *Apsidal Advance Rate*

The apsidal advancc rate may be expressed as

$$\Delta\omega = \frac{\omega_2 - \omega_1 + 360B}{A_n + f} \tag{117}$$

where

$$f = \frac{t_{12} - t_f}{T_{at}} \tag{118}$$

and

B = an intcger chosen by comparing $\Delta\omega$ with the theoretical value computed from the first set of elements, as was done with A of (110).

In cases where no ΔT_a is computed, the A_n value of (112) and $f = 0$ should be used in (117).

Thc advance rate of (117) is expressed in degrees per anomalistie

period, which has direct meaning provided no change in period is calculated. Wbenever ΔT_a is not 0, (117) produces tbe advance rate which when applied to eacb new period* between epocb 1 and epoch 2 results in the motion of perigee from ω_1 to ω_2 as stated in the elements.

X. A COMPUTER-OPERATOR ENSEMBLE FOR ORBIT GENERATION

Computational techniques bave been developed to permit modified orbital elements to be determined initially from the powered flight parameters of the launcb vehicle and subsequently from measured satellite trajectories over a ground station using techniques previously described in this paper. These have been augmented to enable the elements to be refined so as to make them valid for several months and to monitor their validity on a routine basis. The techniques bave been incorporated into five computer programs which have been routinely used, in the case of tbe second TELSTAR satellite, to produce elements for antenna drive tapes, pass scheduling, and satellite attitude predictions. It is the purpose of this section to show the means by which the programs are integrated into a computer-operator system.

10.1 *The Computer Programs*

The five computer programs employed for orbit generation, refinement, and monitoring techniques are:

(*i*) The MOEGEN G3 program
(*ii*) The MOERATE program
(*iii*) Tbe REFINE PERIOD program
(*iv*) The CORD DOPPLER G2 program
(*v*) The MONITOR TAPE ANALYSIS program.

The first four of these were written by the author, while tbe last[22] was basically developed by D. A. Aaronson with certain subroutines by D. A. Ramos. In this section we shall discuss the general function of each program.

10.1.1 *The MOEGEN G3 Program*

The MOEGEN G3 Program generates modified orbital elements for a near-eartb satellite given a list of azimuth, elevation, and, if available, range of tbe satellite as seen from a ground station at specified times. If just these data are used, tbe resulting MOES are said to be free-fit. If the PSI, apsidal advance, and anomalistic period are known from past data, the MOEGEN program may be set to accept these rates along with trajectory information as before and produce a suitable set of MOES.

* A new period is calculated each time the satellite passes through perigee.

These MOES are said to be forced. Since the anomalistic period cannot be accurately determined from a single pass, this latter mode of operation is most valuable in producing elements of long lasting validity.

In addition to generating elements, the MOEGEN program compares trajectories generated from each set of MOES it produces with the points used in the generation, as well as with any additional submitted points from any of the passes from that ground station. Here the program reports azimuth differences, elevation differences, and great circle arc pointing errors as well as range errors. Since the program produces a set of MOES for every group of three azimuth-elevation-range points, these comparisons aid in the selection of the best set of MOES from the group generated. The actual selection, which will be discussed later, is done by an operator, since typically only a few sets of MOES are produced on each generation.

10.1.2 *The MOERATE Program*

The MOERATE program, as its name suggests, refines the PSI, apsidal advance, and period rates along the lines described in Section IX by examining two sets of elements, usually the ones previously in use and the one just generated. In addition, it compares the rates so established to theoretical rates determined from the previous set of MOES using the gravitational theory given in Section VII. In generating rates, higher-order changes beyond the PSI, apsidal advance, and change in period are neglected. For the TELSTAR satellites this omission has resulted in no serious errors in the orbit.

10.1.3 *The REFINE PERIOD Program*

Because computed satellite trajectories are most sensitive to the value calculated for the anomalistic period, the REFINE PERIOD program offers an alternate means for its determination and is particularly valuable before monitor tapes* are available. The program requires a set of MOES and times of meridian crossings from any specified ground station. From each of these it computes an anomalistic period assuming all other element values to be accurate. If there are no errors in the recorded time for each meridian crossing, in the adopted station coordinates, or in the elements, quite naturally all the computed period values should be identical. Any scatter in the computed periods points up errors in the above quantitites. If the meridian crossing times and station locations

* These are magnetic tapes generated at the ground station. They contain, among other data, the measured trajectory of the satellite.

are known to be correct, the scatter acts as a figure of merit for the generated modified orbital elements.

10.1.4 *The CORD DOPPLER G2 Program*

This program accepts either MOES or, in conjunction with a subroutine called MOE, expected burnout parameters for the final powered stage of the satellite launching vehicle. From these it produces an ephemeris for passes over any specified ground station. If burnout quantities are used, the program converts these to MOES, which it prints prior to the ephemeris listing. In addition, this program also produces world maps of the satellite ground trace, drive tapes for both the Andover and Holmdel ground stations, and reports the solar illumination status of the satellite along with a number of communication quantities.

10.1.5 *The MONITOR TAPE ANALYSIS Program*

The monitor tape analysis program written by D. A. Aaronson and described in detail elsewhere[22] compares a satellite trajectory as recorded on a compressed or uncompressed monitor tape[22] to that produced by a set of MOES. Its output is a printed sheet giving great circle arc pointing errors and slant range errors (provided ranging data are present on the monitor tape). It also indicates received microwave carrier power so that one can ascertain whether or not the Andover horn antenna was indeed pointed toward the satellite. This is, of course, essential to proper assessment of the printed errors.

10.2 *Orbital Element Generation Operational Procedures*

The generation of modified orbital elements for the TELSTAR satellites falls into two categories: the initial generation just after launch and the subsequent generation after monitor tapes have become available. Figs. 11 and 12 show the logic operations for these two cases.

10.2.1 *Initial Element Generation*

The initial elements are determined from the expected burnout parameters* of the final powered stage of the launch vehicle. These parameters are based upon the telemetry from the first two stages. Basic

* For the TELSTAR satellites, these have been supplied by J. W. Timko of Bell Laboratories.

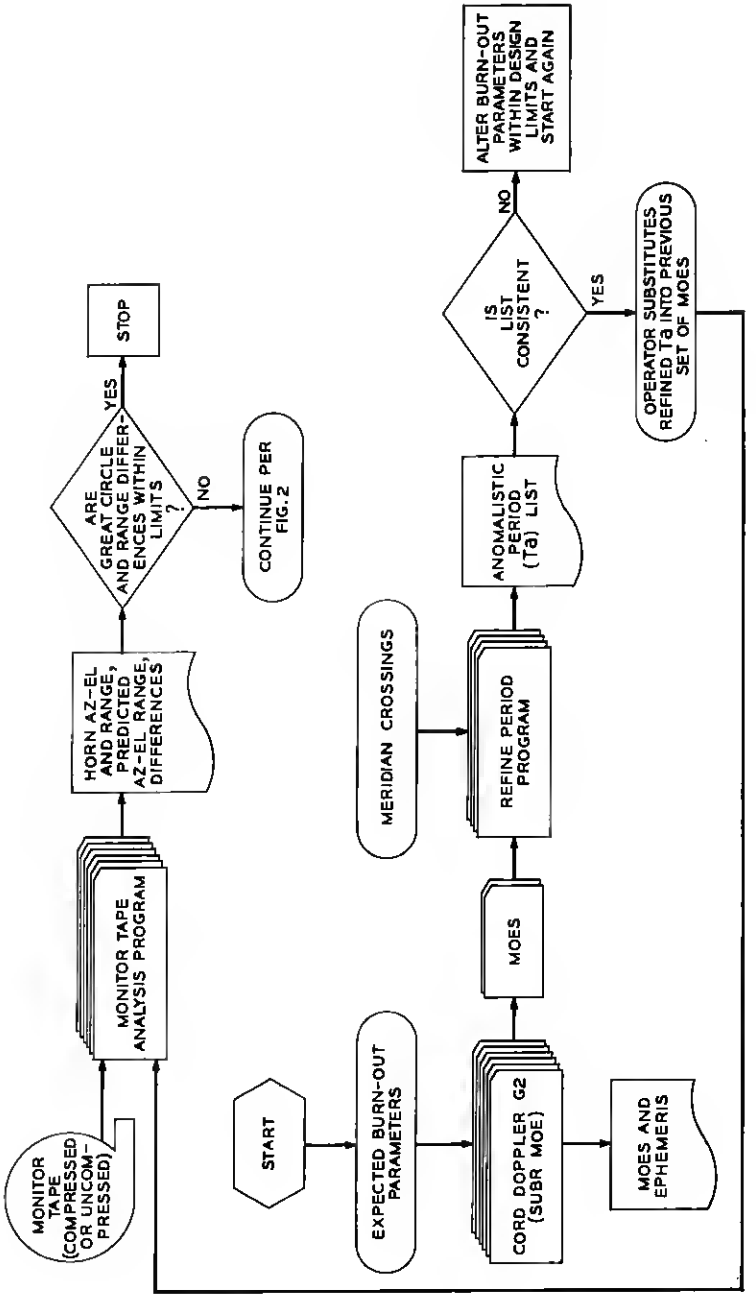

Fig. 11 — Logic blocks for initial modified orbital element generation.

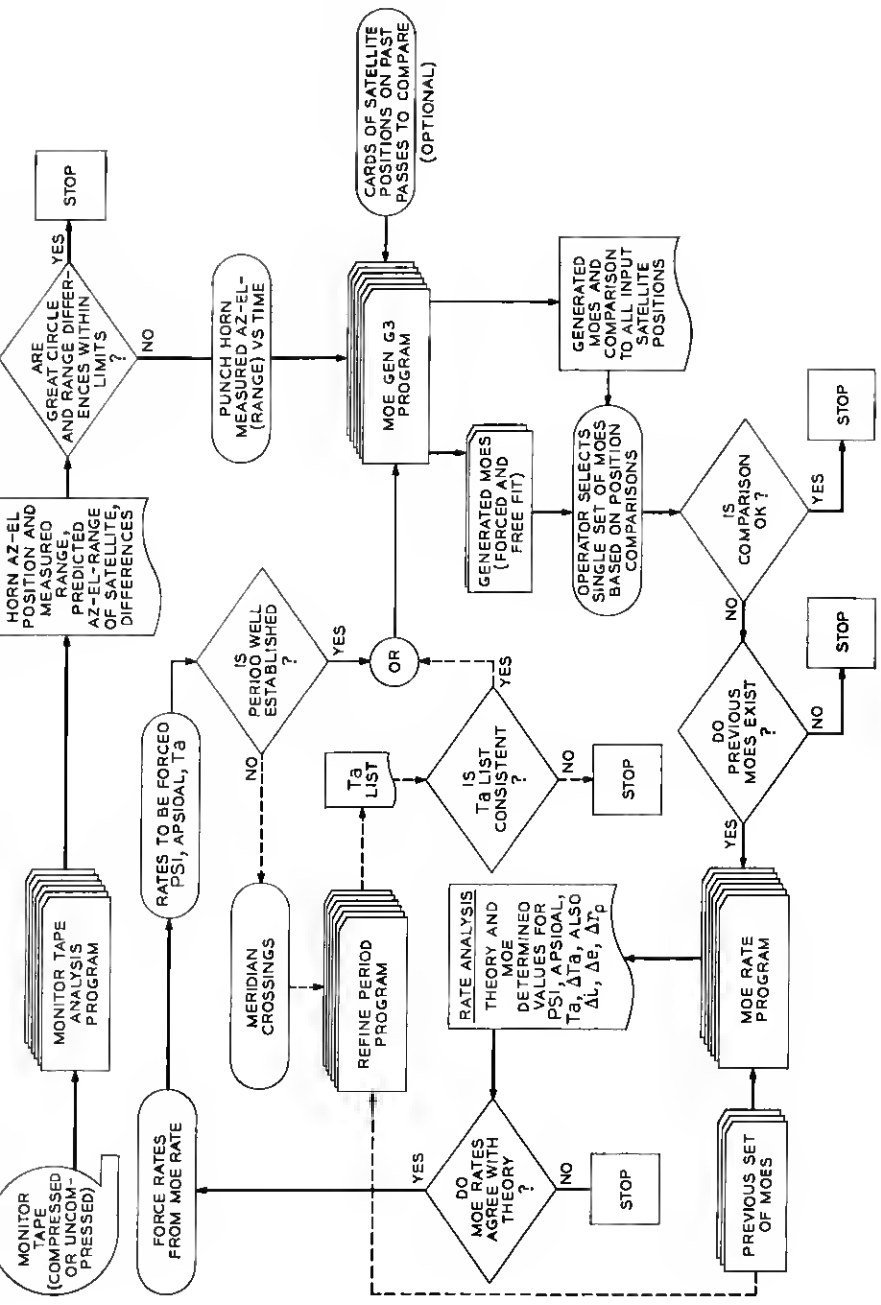

Fig. 12 — Logic blocks for subsequent modified orbital element generation.

to these parameters is the assumption that the third stage performs in a design center manner.

Subroutine MOE of the CORD DOPPLER G2 program accepts the burnout parameters as shown in Fig. 11 and calculates corresponding MOES, which are passed to the main program for ephermeris generation listings.

Modified orbital elements calculated from the burnout parameters are submitted along with subsequent meridian crossings to the REFINE PERIOD program to produce an anomalistic period list as described in Section 10.1.3 (see also Fig. 11). The operator examines this list for consistency. Because the REFINE PERIOD program bases its period calculation on what it assumes as an otherwise correct set of MOES and because the final stage of the launch vehicle, often without telemetry provision, may have performed in a manner different than assumed for orbit generation, it is usually satisfactory to call the period list consistent if the spread of values does not exceed a few tenths of a minute or about 0.1 per cent of the mean anomalistic period for the distribution. If the list is satisfactory according to this criterion, the operator substitutes the mean value of the period into the set of "burnout" MOES and checks minute by minute the predicted trajectory with measured ones by means of the MONITOR TAPE ANALYSIS program as soon as the monitor tape becomes available (see Fig. 11).

Great circle arc errors and range errors reported by the monitor program are scanned by an operator, and if these are within established limits, the element generation process stops and the set of MOES on hand is used for future predictions. If limits are exceeded, the operation proceeds as outlined by Fig. 12, to be discussed later.

Care should be exercised in establishing error criteria for this operator scanning. The first set of MOES, being based on expected burnout parameters, cannot generally produce pointing errors below 0.1° in arc or ± 10 miles in range.

If the anomalistic period list originally generated by the REFINE PERIOD program has too great a spread, an inconsistent set of MOES is generally indicated (see Section 10.1.3). This can occur when the final stage of the launch vehicle departs sufficiently from its design trajectory. It is useful at this time to have on hand a number of MOES generated from burnout parameters with tolerances within the final-stage performance limits. These can be used with the REFINE PERIOD program with the expectation that at least one set will produce an acceptable anomalistic period list. If this procedure is unsuccessful, there

is no recourse but to wait for the monitor tape or sufficient data from tracking stations to establish a correct orbit prediction.

10.2.2 *Subsequent Element Generation*

As soon as monitor tapes become available from Andover, the operation passes into what is termed the subsequent orbital element generation stage. This is outlined in Fig. 12.

As before, monitor tape trajectories are compared to those generated hy the current orbital elements. If these comparisons are unsatisfactory (see Section 10.2.1), the horn azimuth, elevation and the measured range of the satellite along with the corresponding times of measurement are fed to the MOEGEN G3 program. Only a free fit (see Section 10.1.1) is made if no previous rate data are available. Both free and forced fits are made if reasonably reliable values for the prime sweep interval, apsidal advance, and anomalistic period are on band. In the early phases of orbit determination, the REFINE PERIOD program is used to establish an anomalistic period by meridian crossings. After the first workable set of MOES is established by the subsequent generation procedure, the MOERATE program then supplies most of the period values.

In normal operation, the MOEGEN G3 program will compare the input data points to trajectories generated from all output MOES. Optionally, past trajectory data may also be submitted to the program for similar comparisons. An operator scans these comparisons, particularly those concerning the trajectory from which the MOES were derived. The free-fit comparison should have great circle arc differences below 0.05° and range errors below a few miles provided the input trajectory data are consistent with the pointing angles resolved to within 0.02°, as is generally true on the Andover monitor tapes. The forced fit may produce greater errors, which naturally depend on the correctness of the forced data. By these comparisons the operator selects a single set of MOES. Failure to select can occur if input data are excessively noisy or for some reason inconsistent. There is no alternative in this case but to wait for the next monitor tape.

The MOES selected are used directly for future predictions if no previous set other than those from burnout exists. The burnout MOES, being only expected values and having only an approximate epoch, are generally not suitable for submission to the MOERATE program. If a previous set of elements from MOEGEN G3 are available, they are compared to the current set by MOERATE to determine more accurately

the PSI, apsidal advance, and anomalistic period. The operator substitutes these for the earlier rates and again enters MOEGEN G3 using the forced fit mode only. The resulting elements which best fit the present and past trajectories are selected for subsequent use.

XI. TYPICAL EXPERIMENTAL RESULTS

In this section, a typical orbit generation procedure will be illustrated along the lines described in Section 10.2.2 and then a theoretical round-the-world orbit fit will be shown using the techniques of Section VIII. Data for the typical element generation will come from 20 minutes of measurement on each of two passes occurring over Andover on June 30 and July 30. Data from passes on other occasions will be used to determine the accuracy of the predicted trajectories but, for purposes of this illustration, in no way will these latter data be used to refine the orbital elements except as specifically stated.

Fig. 13 shows an output from the MOEGEN G3 program operated in the free-fit mode. Three sets of modified orbital elements were calculated from three data points (azimuth, elevation, range) taken on June 30, 1964. These three sets, shown on lines 7, 8, and 9, differ from each other only in the method of determining the anomalistic period. In the first set, the period is determined from the elements using the perturbation formulations of Section VII. In the second and third sets, the period is determined from the time of flight of the satellite between the data points per Section 6.2.5.

Directly beneath the elements, the program states that the orbit offset is 31.48778°. This is merely an indicator which means that the station is that number of degrees of latitude removed from a point of equal longitude on the orbit plane at the time of the first data point. If this quantity were zero, then the station would be in the orbit plane and this three-point analysis would be invalid.*

The portion of the output enclosed in parentheses displays the comparison of predicted-to-measured trajectories. There are three sets of comparisons, corresponding to the three separate sets of modified orbital elements generated. Here we see that arc and range errors are reasonably small for the June 30 pass (which data were used to determine the elements) but that the fit on June 10, for example, exhibits 5° pointing errors. A survey of the fits clearly indicates that the orbital rates (i.e., prime sweep interval, period, and perigee change) need adjustment.

* Of course the analysis may be rendered invalid if the station is in the orbit plane at the time of *any* of the 3 data points. The first point was reported only as a matter of convenience. In any event the comparison of predicted and measured trajectories described later serves as a final check on the validity of the elements.

Fig. 14 shows the fit of an orbit generated from July 30 data only (azimuth, elevation, range). Here the pointing fit is within 0.02° for that day, but degrades to 0.4° a day later and is grossly inadequate when matched with data from the June 2 trajectories. Again better rate information is needed.

In Fig. 15, we employ the MOERATE program output to determine the orbital rates needed to connect the June 30 and July 30 elements (see Sections IX and 10.1.2). With but a few comments this output should be self-explanatory. First of all, the theoretical values at the bottom of the page are computed from the set of MOES listed at the top left of the figure. The chief purpose for their computation is to gain an estimate of the rates for the actual rate calculations. One cannot compute an average anomalistic period from two given epochs if an estimate of the period is not available. Without such an estimate, the satellite may have made any number of passes through perigee between the two epochs and an infinite array of average periods would be valid solutions. Even with such an estimate, it is sometimes possible to miscalculate the number of times a satellite has passes through perigee if the time between epochs becomes sufficiently large. That is why the number of perigee passes computed by the program is printed out. Fig. 15 (see checked line) has been chosen to show a misestimate of one in the calculation of the perigee passages (= 196) and the attendant error in the average period. By increasing the perigee passes to 197 and performing the indicated division, a new average period of 225.30083 is calculated which is closer to that reported by the first set of MOES and is, of course, a valid solution. Strictly speaking, if this new period value is used, the apsidal advance per T_a should be corrected by multiplying it by 225.30083/226.45032 to obtain $0.19129°/T_a$. The PSI is unaffected by these operations.

Printed at the very bottom of Fig. 15 is the number of iterations required for the computed PSI and apsidal advance rate to come within 2.1 minutes and 0.2 degrees of the theoretical rates. The program stops after 21 iterations whether or not the convergence is successful.

Since there is no reason to suspect that the anomalistic period associated with the June 30 orbit generation possesses high validity (see Fig. 13), the portion of the MOERATE output dealing with changes in period is ignored and the indicated average anomalistic period is used. From Fig. 15, the computed rates become

anomalistic period = 225.30083 minutes
apsidal advance rate = 0.19129° per anomalistic period
prime sweep interval = one day − 8.12511 minutes.

These rates are then submitted along with the June 30 data to MOE-

```
MOEGEN G3 - ORBIT GENERATION FROM ANOOVER TRAJECTORIES  - L C THOMAS *

RANGE DATA SUPPLIED ON ALL THREE POINTS.     FREE FIT

REFRACTION CORRECTION APPLIED TO INPUT AND OUTPUT SATELLITE ELEVATIONS.

COMPUTED MODIFIED ORBITAL ELEMENTS-

POINT  TER        E P O C H          INCL     ASC   NODE PSI 10AY-  ARG PERIG  PERIGEE CHG  ANOM  PERIOD  PER)OD CHG ECCEN-   RAD PERIGEE
 NO     NO  YEAR MO DY HR MINUTE   DEGREES   WEST LONG   MINUTES       DEG        DEG/DA        MIN        MIN/PERIOD TRICITY  STAT MILES

  1      4  1964  6 30  2 53.962  42.76190  219.33549  -8.15271  322.80277   0.19015    225.33698     0.       0.40079     4567.911
            1964  6 30  2 54.019            219.34985            322.80277   0.19015    225.24235  FROM DATA POINT 1 TO 2 TIME
            1964  6 30  2 54.011            219.34777            322.80277   0.19014    225.25611  FROM DATA POINT 1 TO 3 TIME
   ORBIT OFFSET =   31.48778 DEG OF LAT.  IF 0 1ST SUBSAT POINT IN ORBIT PLANE.


          IYEAR MO DY HR MN SEC  (   POINTING ANGLE COMPARISON - STATION AT ANOOVER ME    )
                                 (   M-E-A-S-U-R-E-O          P-R-E-D-1-C-7-E-O      O  I  F  F  E  R  E  N  C  E  S  )
                                  AZ-DEG EL-DEG RANGE-MI AZ-DEG EL-DEG RANGE-MI AZ-DIFF EL-DIFF ARC-DIF RANGE-DIFF)
          I1964  6 30  5 10 -0   210.36  37.45  7446.59 210.36  37.43  7446.58  -0.000   0.021   0.0232    0.008 )
          I1964  6 30  5 20 -0   201.69  31.35  7347.55 201.68  31.32  7347.45   0.007   0.030   0.0328    0.098 )
          I1964  6 30  5 30 -0   193.71  23.77  7214.50 193.70  23.72  7214.50   0.010   0.049   0.0514    0.003 )
          I1964  6  2  3 40 -0   275.88  25.01  6175.84 274.88  36.37  6146.51   0.997 -11.359  11.3911   29.333 )
          I1964  6  2  3 42 -0   275.94  27.96  6186.80 274.87  39.10  6171.00   1.070 -11.139  11.1741   15.800 )
          I1964  6  2  3 44 -0   275.97  30.83  6201.62 274.82  41.75  6197.83   1.146 -10.922  10.9610    3.786 )
          I1964  6 10  7 52 -0   280.67  27.72  8247.93 276.31  30.46  8108.94   4.359  -2.744   4.6934  138.989 )
          I1964  6 10  8  0 -0   274.59  30.17  8101.17 269.69  32.47  7939.42   4.897  -2.299   4.7722  161.752 )
          I1964  6 10  8 10 -0   266.01  32.14  7859.83 260.38  33.81  7670.60   5.634  -1.668   5.0113  189.228 )
          I1964  7 30 23 10 -0   287.17  15.74  4461.54 259.38  33.86  7640.36  27.789 -18.120  30.8822-3178.820 )
          I1964  7 30 23 20 -0   270.42  37.43  4523.82 284.27  20.57  4527.54 -13.854  16.861  20.7102   -3.720 )
          I1964  7 30 23 30 -0   246.88  49.81  4987.65 266.37  39.59  4710.35 -19.488  10.221  17.1299  277.295 )
          I1964  8  1  1 50 -0   272.56  17.52  6562.70 283.67  10.20  6368.05 -11.109   7.321  13.0277  194.653 )
          I1964  8  1  2 10 -0   260.38  21.80  7043.55 271.05  17.13  6787.11 -10.670   4.669  11.0863  256.444 )
          I1964  8  1  2 10 -0   249.56  23.23  7537.26 259.51  20.57  7270.91  -9.951   2.658   9.6049  266.352 )
```

Fig. 13 — Output from the MOEGEN G3 program operated in the free-fit mode. June 30 data only.

YEAR	MO	DY	HR	MN	SEC	POINTING ANGLE COMPARISON - STATION AT ANDOVER ME										
						M-E-A-S-U-R-E-D			P-R-E-D-I-C-T-E-D			O-I-F	F-F-E-R-E-N-C-E-S			
						AZ-DEG	EL-DEG	RANGE-MI	AZ-DEG	EL-DEG	RANGE-MI	AZ-DIFF	EL-DIFF	ARC-DIF	RANGE-DIFF	
1964	6	30	5	10	0	210.36	37.45	7446.59	210.36	37.43	7446.58	-0.000	0.021	0.0232	0.008	
1964	6	30	5	20	0	201.69	31.35	7347.55	201.68	31.32	7347.39	0.012	0.033	0.0343	0.164	
1964	6	30	5	30	0	193.71	23.77	7214.50	193.69	23.71	7214.35	0.019	0.056	0.0581	0.146	
1964	6	2	3	40	0	275.88	25.01	6175.84	276.88	6.73	6314.68	-0.996	18.284	18.3091	-138.845	
1964	6	2	3	42	0	275.94	27.96	6186.80	277.00	10.00	6295.31	-1.060	17.962	17.9892	-108.510	
1964	6	2	3	44	0	275.97	30.83	6201.62	277.11	13.21	6282.42	-1.141	17.617	17.6485	-80.800	
1964	6	10	7	52	0	280.67	27.72	8247.93	286.49	23.52	8418.33	-5.820	4.198	6.7188	-170.400	
1964	6	10	8	0	0	274.59	30.17	8101.17	281.09	26.56	8308.63	-6.495	3.610	6.7579	-207.456	
1964	6	10	8	10	0	266.01	32.14	7859.83	273.45	29.37	8114.22	-7.444	2.771	6.9692	-254.388	
1964	7	30	23	10	0	287.17	15.74	4461.54	265.68	42.63	4483.39	21.493	-26.890	32.5807	-21.850	
1964	7	30	23	20	0	270.42	37.43	4523.82	239.53	53.35	5007.64	30.895	-15.916	26.5686	-483.820	
1964	7	30	23	30	0	246.88	49.81	4987.65	213.85	54.25	5676.42	33.029	-4.437	20.5984	-688.773	
1964	8	1	1	50	0	272.56	17.52	6562.70	256.18	24.51	7019.15	16.375	-6.988	16.7892	-456.452	
1964	8	1	2	0	0	260.38	21.80	7043.55	245.28	25.40	7515.27	15.100	-3.598	14.2879	-471.716	
1964	8	1	2	10	0	249.56	23.23	7537.26	235.92	24.41	7971.31	13.639	-1.175	12.5275	-434.046	

YEAR	MO	DY	HR	MN	SEC	POINTING ANGLE COMPARISON - STATION AT ANDOVER ME										
						M-E-A-S-U-R-E-D			P-R-E-D-I-C-T-E-D			O-I-F	F-F-E-R-E-N-C-E-S			
						AZ-DEG	EL-DEG	RANGE-MI	AZ-DEG	EL-DEG	RANGE-MI	AZ-DIFF	EL-DIFF	ARC-DIF	RANGE-DIFF	
1964	6	30	5	10	0	210.36	37.45	7446.59	210.36	37.43	7446.58	-0.000	0.021	0.0221	0.008	
1964	6	30	5	20	0	201.69	31.35	7347.55	201.68	31.32	7347.40	0.011	0.032	0.0350	0.155	
1964	6	30	5	30	0	193.71	23.77	7214.50	193.69	23.72	7214.38	0.018	0.055	0.0564	0.125	
1964	6	2	3	40	0	275.88	25.01	6175.84	276.64	11.24	6261.92	-0.755	13.766	13.7846	-86.080	
1964	6	2	3	42	0	275.94	27.96	6186.80	276.75	14.46	6250.84	-0.807	13.503	13.5234	-64.039	
1964	6	2	3	44	0	275.97	30.83	6201.62	276.85	17.60	6245.66	-0.875	13.230	13.2543	-44.041	
1964	6	10	7	52	0	280.67	27.72	8247.93	285.13	24.60	8378.68	-4.460	3.116	5.0721	-130.747	
1964	6	10	8	0	0	274.59	30.17	8101.17	279.57	27.51	8260.32	-4.981	2.662	5.1101	-159.152	
1964	6	10	8	10	0	266.01	32.14	7859.83	271.72	30.13	8054.81	-5.707	2.012	5.2823	-194.983	
1964	7	30	23	10	0	287.17	15.74	4461.54	271.97	37.08	4420.90	15.205	-21.338	25.2349	40.639	
1964	7	30	23	20	0	270.42	37.43	4523.82	248.00	50.83	4863.19	22.419	-13.397	20.7917	-339.368	
1964	7	30	23	30	0	246.88	49.81	4987.65	221.57	54.22	5503.08	25.308	-4.406	16.0897	-515.429	
1964	8	1	1	50	0	272.56	17.52	6562.70	260.10	23.19	6909.71	12.457	-5.675	12.9757	-347.006	
1964	8	1	2	0	0	260.38	21.80	7043.55	248.87	24.80	7408.11	11.514	-3.001	10.9882	-364.562	
1964	8	1	2	10	0	249.56	23.23	7537.26	239.15	24.31	7876.25	10.407	-1.082	9.5826	-338.990	

ABOVE ELEMENTS COMPUTED FROM POINTING ANGLES
AND SLANT RANGES
FROM ANDOVER ME LAT 44.63550 DEG WEST LONG 70.70030 DEG MEAN ABOVE MSL 945.00000 FT

Fig. 13 (cont.).

```
MBEGEN G3 - BRBIT GENERATION FROM ANDOVER TRAJECTORIES  - L C THOMAS *

RANGE DATA SUPPLIED ON ALL THREE POINTS.      FREE FIT

REFRACTION CORRECTION APPLIED TO INPUT AND OUTPUT SATELLITE ELEVATIONS.

COMPUTED MODIFIED BRBITAL ELEMENTS-

POINT ITER       E P B C H          INCL     ASC  NODE PS1 IDAY- ARG PERIG PERIGEE CHG ANOM PERIOD PERIOD CHG ECCEN-  RAD PERIGEE
 NO    NO  YEAR MO DY HR MINUTE   DEGREES   WEST LONG   MINUTES     DEG      DEG/TA        MIN      MIN/PERIOD TRICITY  STAT MILES

  1     4  1964  7 30 22 38.226  42.74888 218.36545  -8.15854   0.48840   0.19044    225.26541     0.          0.40101    4565.221
           1964  7 30 22 38.235            218.36768              0.48840   0.19041    225.20241 FROM DATA POINT 1 TO 2 TIME
           1964  7 30 22 38.239            218.36886              0.48840   0.19044    225.16912 FROM DATA POINT 1 TO 3 TIME
    BRBIT OFFSET =     2.12031 DEG OF LAT.  IF O 1ST SUBSAT POINT IN BRBIT PLANE.


          (YEAR MO DY HR MN SEC  (   POINTING ANGLE COMPARISON - STATION AT ANDOVER ME   )
                                 |   M-E-A-S-U-R-E-O        P-R-E-D-I-C-T-E-O     O I F F  E R E N C E S I
                                 AZ-DEG EL-DEG RANGE-MI AZ-DEG EL-DEG RANGE-MI AZ-DIFF EL-DIFF ARC-DIF RANGE-DIFF)
          (1964  7 30 23 10 -0  287.17  15.74  4461.54 287.17  15.74  4461.54    0.      0.000    0.0001    0.003 )
          (1964  7 30 23 20 -0  270.42  37.43  4523.82 270.41  37.44  4523.87   0.007   -0.006    0.0140   -0.054 )
          (1964  7 30 23 30 -0  246.88  49.81  4987.65 246.86  49.80  4987.97   0.017    0.010    0.0185   -0.319 )
          (1964  6  2  3 40 -0  275.88  25.01  6175.84 276.93   2.00  6362.61  -1.046   23.011  23.0332 -186.765 )
          (1964  6  2  3 42 -0  275.94  27.96  6186.80 277.06   5.26  6333.38  -1.121   22.701  22.7258 -146.577 )
          (1964  6  2  3 44 -0  275.97  30.83  6201.62 277.18   8.54  6311.29  -1.214   22.292  22.3210 -109.666 )
          (1964  6 10  7 52 -0  280.67  27.72  8247.93 289.19  21.28  8483.61  -8.522    6.435  10.0705 -235.682 )
          (1964  6 10  8  0 -0  274.59  30.17  8101.17 284.09  24.62  8394.27  -9.500    5.547  10.0888 -293.102 )
          (1964  6 10  8 10 -0  266.01  32.14  7859.83 276.90  27.84  8226.51 -10.890    4.305  10.3611 -366.684 )
          (1964  6 30  5 10 -0  210.36  37.45  7446.59 218.99  39.86  7524.03  -8.627   -2.409   7.1512  -77.435 )
          (1964  6 30  5 20 -0  201.69  31.35  7347.55 209.66  34.97  7452.25  -7.968   -3.618   7.5854 -104.703 )
          (1964  6 30  5 30 -0  193.71  23.77  7214.50 201.16  28.59  7335.52  -7.454   -4.822   8.2423 -121.015 )
          (1964  8  1  1 50 -0  272.56  17.52  6562.70 272.21  17.72  6571.79   0.354   -0.195   0.3898   -9.088 )
          (1964  8  1  2  0 -0  260.38  21.80  7043.55 260.05  21.87  7054.06   0.332   -0.071   0.3160  -10.507 )
          (1964  8  1  2 10 -0  249.56  23.23  7537.26 249.25  23.24  7547.68   0.306   -0.008   0.2819  -10.420 )
```

Fig. 14 — Fit of orbit generated from July 30 data only.

YEAR	MØ	DY	HR	MN	SEC	M-E-A-S-U-R-E-D A2-DEG	M-E-A-S-U-R-E-D EL-DEG	M-E-A-S-U-R-E-D RANGE-MI	P-R-E-D-I-C-T-E-D A2-DEG	P-R-E-D-I-C-T-E-D EL-DEG	P-R-E-D-I-C-T-E-D RANGE-MI	D I F F E R E N C E S A2-DIFF	D I F F E R E N C E S EL-DIFF	D I F F E R E N C E S ARC-DIFF	D I F F E R E N C E S RANGE-DIFF
1964	7	30	23	10	-0	287.17	15.74	4461.54	287.17	15.74	4461.54	0.	0.000	0.0001	0.003
1964	7	30	23	20	-0	270.42	37.43	4523.82	270.41	37.44	4523.93	0.013	-0.012	0.0156	-0.112
1964	7	30	23	30	-0	246.88	49.81	4987.65	246.85	49.81	4988.25	0.034	0.005	0.0242	-0.604
1964	6	2	3	40	-0	275.88	25.01	6175.84	244.27	50.47	5047.31	31.611	-25.463	35.1858	1128.529
1964	6	2	3	42	-0	275.94	27.96	6186.80	277.06	5.26	6333.38	-1.121	22.701	22.7258	-146.577
1964	6	2	3	44	-0	275.97	30.83	6201.62	277.18	8.54	6311.29	-1.214	22.292	22.3210	-109.666
1964	6	10	7	52	-0	280.67	27.72	8247.93	302.51	6.45	8770.53	-21.837	21.272	29.6863	-522.599
1964	6	10	8	0	-0	274.59	30.17	8101.17	298.54	11.24	8770.14	-23.952	18.935	29.2067	-668.971
1964	6	10	8	10	-0	266.01	32.14	7859.83	293.12	16.29	8725.96	-27.105	15.846	29.2219	-866.133
1964	6	30	5	10	-0	210.36	37.45	7446.59	236.22	41.29	7629.98	-25.861	-3.845	20.2789	-183.387
1964	6	30	5	20	-0	201.69	31.35	7347.55	225.97	38.76	7614.93	-24.284	-7.406	21.1351	-267.378
11964	6	30	5	30	-0	193.71	23.77	7214.50	216.48	34.64	7544.05	-22.771	-10.875	22.5774	-329.551
1964	8	1	1	50	-0	272.56	17.52	6562.70	271.56	18.07	6586.90	1.000	-0.552	1.1005	-24.202
1964	8	1	2	0	-0	260.38	21.80	7043.55	259.44	22.08	7071.41	0.943	-0.282	0.9194	-27.857
1964	8	1	2	10	-0	249.56	23.23	7537.26	248.69	23.34	7564.66	0.870	-0.109	0.8071	-27.400

YEAR	MØ	DY	HR	MN	SEC	M-E-A-S-U-R-E-D A2-DEG	M-E-A-S-U-R-E-D EL-DEG	M-E-A-S-U-R-E-D RANGE-MI	P-R-E-D-I-C-T-E-D A2-DEG	P-R-E-D-I-C-T-E-D EL-DEG	P-R-E-D-I-C-T-E-D RANGE-MI	D I F F E R E N C E S A2-DIFF	D I F F E R E N C E S EL-DIFF	D I F F E R E N C E S ARC-DIFF	D I F F E R E N C E S RANGE-DIFF
1964	7	30	23	10	-0	287.17	15.74	4461.54	287.17	15.74	4461.54	0.	0.000	0.0001	0.003
1964	7	30	23	20	-0	270.42	37.43	4523.82	270.40	37.44	4523.96	0.016	-0.015	0.0198	-0.143
1964	7	30	23	30	-0	246.88	49.81	4987.65	246.84	49.81	4988.40	0.042	0.002	0.0280	-0.754
1964	6	2	3	40	-0	275.88	25.01	6175.84	244.26	50.48	5047.48	31.620	-25.466	35.1922	1128.365
1964	6	2	3	42	-0	275.94	27.96	6186.80	277.06	5.26	6333.38	-1.121	22.701	22.7258	-146.577
11964	6	2	3	44	-0	275.97	30.83	6201.62	277.18	8.54	6311.29	-1.214	22.292	22.3210	-109.666
1964	6	10	7	52	-0	280.67	27.72	8247.93	302.51	6.45	8770.53	-21.837	21.272	29.6863	-522.599
1964	6	10	8	0	-0	274.59	30.17	8101.17	305.16	3.06	8874.56	-30.572	27.107	39.6325	-773.389
1964	6	10	8	10	-0	266.01	32.14	7859.83	300.25	9.01	8885.91	-34.236	23.135	39.2245	-1026.076
1964	6	30	5	10	-0	210.36	37.45	7446.59	245.22	40.62	7663.65	-34.855	-3.168	27.0812	-217.061
1964	6	30	5	20	-0	201.69	31.35	7347.55	234.81	39.35	7681.38	-33.117	-7.996	27.9938	-333.833
11964	6	30	5	30	-0	193.71	23.77	7214.50	224.95	36.44	7641.36	-31.238	-12.673	29.6687	-426.856
11964	8	1	1	50	-0	272.56	17.52	6562.70	271.22	18.26	6594.96	1.341	-0.738	1.4742	-32.264
11964	8	1	2	0	-0	260.38	21.80	7043.55	259.11	22.19	7080.60	1.266	-0.391	1.2376	-37.046
11964	8	1	2	10	-0	249.56	23.23	7537.26	248.39	23.39	7573.62	1.168	-0.161	1.0846	-36.358

ABOVE ELEMENTS COMPUTED FROM POINTING ANGLES
AND SLANT RANGES
FROM ANDOVER ME LAT 44.63550 DEG WEST LONG 70.70030 DEG HT ABOVE MSL 945.00000 FT

Fig. 14 (cont.).

```
TELSTAR II - RATE GENERATION FROM DUAL ODE SETS          L C THOMAS

COMPARISON FOR ALL THREE RANGE VALUES SUPPLIED.


RATES TO FOLLOW BASED ON FOLLOWING PAIR OF MODIFIED ORBITAL ELEMENTS-

 REFERENCE TIME              1964  JUNE 30   2 HR  53.96210 MIN UT     1964  JULY 30  22 HR  38.22600 MIN UT
 INCLINATION                   42.76190 DEG                             42.74888 DEG
 ASCENDING NODE (WEST LONG)   219.33549 DEG                            218.36545 DEG
 PRIME SWEEP INTERVAL  ONE DAY  -8.15271 MIN                            -8.15854 MIN
 PERIGEE AND SATELLITE POSITION 322.80277 DEG                             0.48840 DEG
    RATE OF CHANGE              0.19015 DEG/TA                           0.19044 DEG/TA
 ANOMALISTIC PERIOD           225.33698 MIN                            225.26541 MIN
    RATE OF CHANGE               0.          MIN/TA                      0.          MIN/TA
 ECCENTRICITY                  0.400788                                 0.401010
 RADIUS OF PERIGEE          4567.91095 STATUTE MILES                 4565.22095 STATUTE MILES

RATES CALCULATED FROM ABOVE ELEMENTS ARE

 PRIME SWEEP INTERVAL  ONE DAY   -8.12511 MIN
 APSIDAL ADVANCE    0.19227 DEG/TA
 CHANGE IN ANOMALISTIC PERIOD 0.011360648 MIN/TA (PROVIDED ANOMALISTIC PERIOD OF INITIAL NODE SET IS CORRECT)
 ANOMALISTIC PERIOD OF INITIAL NODE SET =  225.33698 MIN

 INCLINATION CHANGE -0.000066 DEG/TA
 ECCENTRICITY CHANGE 0.00000113 UNITS/TA
 RADIUS OF PERIGEE CHANGE   -0.01372 STATUTE MI/TA

ABOVE RATES APELIED TO FIRST SET OF NODES LISTED ABOVE WILL YIELD SECOND NODE SET.


FOLLOWING RATES APPLY IF GIVEN NODES CONNECTED WITH SINGLE ANOM PERIOD AND ZERO RATE OF CHANGE-

RATES CALCULATED FOR ABOVE ELEMENTS ARE

 PRIME SWEEP INTERVAL  ONE DAY   -8.12511 MIN
 APSIDAL ADVANCE    0.19227 DEG/TA (0.19129 DEG/TA, SEE TEXT)
 CHANGE IN ANORALISTIC PERIOD 0.          MIN/TA
 ANOMALISTIC PERIOD = TIME BETWEEN NODE EPOCHS/CAL NUMBER OF PERIGEE PASSES =  44384.263 / 196.00
                    = 226.45032 MIN (225.300827 MIN, SEE TEXT)

 INCLINATION CHANGE -0.000066 DEG/TA
 ECCENTRICITY CHANGE 0.00000113 UNITS/TA
 RADIUS OF PERIGEE CHANGE   -0.01372 STATUTE MI/TA

ABOVE RATES APPLIED TO FIRST SET OF NODES LISTED ABOVE WILL YIELD SECOND NODE SET.


THEORETICAL VALUES FOLLOW-
 REPUERIAN PERIOD= 225.38766 MIN
 NODAL PERIOD= 225.29030 MIN
 ANOMALISTIC PERIOD= 225.33692 MIN
 PRIME SWEEP INTERVAL= 1 DAY-8.15271 MIN
 APSIDAL ADVANCE= 0.19015 DEG/TA

ITERATIONS FOR PSI=  1
ITERATIONS FOR APSIDAL ADVANCE=  2
```

Fig. 15 — Orbital rate generation.

GEN G3. The output is shown in Fig. 16. A considerable improvement in the fit over the June 2 to August 1 period is seen, with the bulk of the errors within the low hundredths of degree range. A maximum range error of only 7 miles over this interval is also noted.

Even these small errors may indicate the need for additional orbital rate improvement. The mean rates determined by combining June 2, 10, 30 and July 30 data are

anomalistic period = 225.30049 minutes
apsidal advance rate = 0.19105° per anomalistic period
prime sweep interval = one day − 8.12480 minutes.

Using these rates produces an even better trajectory fit, as shown in Fig. 17. The mere fact that the maximum measured error is about 0.05° and within five miles in range over a 3-month period indicates the near constancy of the secular rates and attests to the fact that little energy is being lost by the satellite as it orbits.

Fig. 18 illustrates the end result of the same type of procedure as described above, except that only one range point per determination is used in the generation. Here the pointing errors peak at 0.6° over the survey with maximum range errors about 25 miles.*

Fig. 19 repeats the above with absolutely no range data fed to the orbital generation process. Over the survey, maximum pointing and range errors are 0.8° and 76 miles respectively.

The advantage of 3 range points per determination over the several months' survey period is clearly evident by the results.

It must be stated that this illustrative example is somewhat simplified in that a certain amount of initial, free-fit orbit generation is omitted. In actual operation, the free-fit mode of MOEGEN G3 is often run for 6 to 12 data points in various combinations, and only the elements producing the best trajectory fit are preserved for later rate processing.

At this point, we intend to show how the techniques of Section VIII will provide a better round-the-world orbit fit by modifying the eccentricity and perigee radius of the orbital elements. Since no data pertaining to the TELSTAR satellites were readily obtainable from stations in southern latitudes, it was decided to proceed as described below.

A set of orbital elements† (which we shall call MO) was generated

* The −7449.740 and −7211.212 range "errors" indicated by Fig. 18 are not true errors but merely reflect the fact that no range data were supplied at these times for generation purposes. The true errors are ±3 miles, as shown several lines below.

† These orbital elements had previously predicted Andover passes to a pointing accuracy of 0.07°.

```
MOEGEN G3 - ORBIT GENERATION FROM ANOOVER TRAJECTORIES - L C THOMAS *

3 POINT RANGE DATA SUPPLIED.  FIT FORCED IO JUNE 30 - JULY 30 RATES.

REFRACTION CORRECTION APPLIED TO INPUT AND OUTPUT SATELLITE ELEVATIONS.

COMPUTED MODIFIED ORBITAL ELEMENTS-

POINT ITER      E P O C H          INCL     ASC  NOOE PSI 1DAY- ARG PERIG PERIGEE CHG ANOM PERIOO PERIOO CHG ECCEN-  RAD PERIGEE
 NO    NO  YEAR MO DY HR MINUTE  DEGREES  WEST LONG  MINUTES     DEG      DEG/TA       MIN      MIN/PERIOO 7RICITY  STA7 MILES

  1     4  1964  6 30  2 53.984  42.76212 219.34173  -8.12511 322.80221   0.19129    225.30083     0.       0.40079    4567.873
           1964  6 30  2 54.019           219.35058           322.80221   0.19124    225.24250 FROM DATA POINT 1 TO 2 TIME
           1964  6 30  2 54.011           219.34851           322.80221   0.19125    225.25618 FROM DATA POINT 1 TO 3 TIME
   ORBIT OFFSET =   31.48778 DEG OF LAT.  (F O 1ST SUBSAT POINT IN ORBIT PLANE.

          (YEAR MO DY HR MN SEC  (   POINTING ANGLE COMPARISON - STATION AT ANOOVER ME   )
                                 (   M-E-A-S-U-R-E-O          P-R-E-O-(-C-7-E-O     O 1 F F E R E N C E S )
                                  AZ-DEG EL-DEG RANGE-MI AZ-DEG EL-DEG RANGE-MI AZ-DIFF EL-DIFF ARC-DIF RANGE-DIFF)
          (1964  6 30  5 10 -0  210.36  37.45  7446.59 210.36  37.43  7446.58  -0.000   0.021   0.0232    0.008 )
          (1964  6 30  5 20 -0  201.69  31.35  7347.55 201.68  31.32  7347.43   0.009   0.031   0.0343    0.124 )
          (1964  6 30  5 30 -0  193.71  23.77  7214.50 193.70  23.72  7214.44   0.013   0.052   0.0533    0.058 )
          (1964  6  2  3 40 -0  275.88  25.01  6175.84 275.90  25.06  6182.44  -0.022  -0.045   0.0490   -6.596 )
          (1964  6  2  3 42 -0  275.94  27.96  6186.80 275.96  28.00  6193.38  -0.021  -0.040   0.0442   -6.583 )
          (1964  6  2  3 44 -0  275.97  30.83  6201.62 276.00  30.87  6208.18  -0.029  -0.036   0.0437   -6.564 )
          (1964  6 10  7 52 -0  280.67  27.72  8247.93 280.69  27.73  8248.67  -0.017  -0.008   0.0198   -0.742 )
          (1964  6 10  8  0 -0  274.59  30.17  8101.17 274.60  30.18  8101.09  -0.015  -0.009   0.0156    0.079 )
          (1964  6 10  8 10 -0  266.01  32.14  7859.83 266.01  32.13  7858.74  -0.002   0.014   0.0198    1.093 )
          (1964  7 30 23 10 -0  287.17  15.74  4461.54 287.25  15.65  4464.80  -0.080   0.087   0.1166   -3.258 )
          (1964  7 30 23 20 -0  270.42  37.43  4523.82 270.53  37.37  4524.75  -0.114   0.062   0.1097   -0.932 )
          (1964  7 30 23 30 -0  246.88  49.81  4987.65 247.01  49.78  4987.17  -0.135   0.035   0.0944    0.484 )
          (1964  8  1  1 50 -0  272.56  17.52  6562.70 272.63  17.50  6562.56  -0.066   0.017   0.0660    0.136 )
          (1964  8  1  2  0 -0  260.38  21.80  7043.55 260.44  21.75  7043.18  -0.060   0.047   0.0727    0.370 )
          (1964  8  1  2 10 -0  249.56  23.23  7537.26 249.61  23.19  7536.95  -0.047   0.042   0.0602    0.313 )

ABOVE ELEMENTS COMPUTED FROM POINTING ANGLES
AND SLANT RANGES
FROM ANOOVER ME   LAT   44.63550 DEG  WEST LONG   70.70030 DEG  HT ABOVE MSL  945.00000 FT
```

Fig. 16 — Fit obtained by combining July 30 and June 30 data.

MEEGEN G3 - ØRBIT GENERATIØN FRØM ANOØVER TRAJECTØRIES - L C THØMAS *

RANGE DATA SUPPLIED ØN ALL THREE PØINTS. FØRCED FIT (AVERAGE RATES)

REFRACTIØN CØRRECTIØM APPLIED TØ INPUT AND ØUTPUT SATELLITE ELEVATIØNS.

CØMPUTED MØDIFIED ØRBITAL ELEMENTS-

PØINT ME	ITER MØ	E P Ø C H YEAR MØ ØY HR MINUTE	INCL DEGREES	ASC NØDE PSI 1ØAY- WEST LØNG MINUTES	ARG PERIG ØEG	PERIGEE CHG ØFG/TA	ANØM PERIØD MIN	PERIØD CHG MIN/PERIØD	ECCEN- TRICITY	RAD PERIGEE STAT MILES
1	4	1964 6 30 2 53.984	42.76210	219.34180 -8.12480	322.80243	0.19105	225.30049	0.	0.40079	4567.869
		1964 6 30 2 54.020		219.35069	322.80243	0.19100	225.24189	FRØM ØATA PØINT 1 TØ 2		TIME
		1964 6 30 2 54.011		219.34859	322.80243	0.19101	225.25576	FRØM ØATA PØINT 1 TØ 3		TIME

ØRBIT ØFFSET = 31.48778 DEG ØF LAT. IF 0 1ST SUBSAT PØINT IN ØRBIT PLANE.

(YEAR MØ ØY HR MN SEC	(PØINTING ANGLE CØMPARISØN - STATIØN AT ANØØVER ME) (M-E-A-S-U-R-E-D P-R-E-D-I-C-T-E-D O 1 F F E R E N C E S) AZ-ØEG EL-ØEG RANGE-MI	AZ-ØEG EL-DEG RANGE-MI	AZ-DIFF EL-DIFF ARC-DIF RANGE-DIFF)
(1964 6 30 5 10 -0	210.36 37.45 7446.59	210.36 37.43 7446.58	-0.000 0.021 0.0221 0.008)
(1964 6 30 5 20 -0	201.69 31.35 7347.55	201.68 31.32 7347.43	0.009 0.031 0.0343 0.124)
(1964 6 30 5 30 -0	193.71 23.77 7214.50	193.70 23.72 7214.44	0.013 0.052 0.0537 0.058)
(1964 6 2 3 40 -0	275.88 25.01 6175.84	275.91 25.00 6180.25	-0.026 0.005 0.0242 -4.407)
(1964 6 2 3 42 -0	275.94 27.96 6186.80	275.97 27.95 6191.13	-0.026 0.008 0.0252 -4.327)
(1964 6 2 3 44 -0	275.97 30.83 6201.62	276.00 30.82 6205.87	-0.033 0.008 0.0305 -4.247)
(1964 6 10 7 52 -0	280.67 27.72 8247.93	280.69 27.73 8248.71	-0.020 -0.006 0.0185 -0.784)
(1964 6 10 8 0 -0	274.59 30.17 8101.17	274.61 30.18 8101.52	-0.017 -0.008 0.0185 -0.352)
(1964 6 10 8 10 -0	266.01 32.14 7859.83	266.02 32.13 7859.67	-0.006 0.015 0.0198 0.162)
(1964 7 30 23 10 -0	287.17 15.74 4461.54	287.19 15.78 4465.22	-0.019 -0.042 0.0448 -3.676)
(1964 7 30 23 20 -0	270.42 37.43 4523.82	270.46 37.45 4527.84	-0.037 -0.024 0.0389 -4.023)
(1964 7 30 23 30 -0	246.88 49.81 4987.65	246.93 49.81 4991.24	-0.053 -0.004 0.0370 -3.592)
(1964 8 1 1 50 -0	272.56 17.52 6562.70	272.59 17.54 6566.02	-0.027 -0.018 0.0313 -3.324)
(1964 8 1 2 0 -0	260.38 21.80 7043.55	260.41 21.77 7046.47	-0.032 0.027 0.0408 -2.920)
(1964 8 1 2 10 -0	249.56 23.23 7537.26	249.59 23.20 7539.72	-0.028 0.029 0.0396 -2.461)

ABØVE ELEMENTS CØMPUTED FRØM PØINTING ANGLES
AND SLANT RANGES
FRØM ANCØVER ME LAT 44.63550 DEG WEST LØNG 70.70030 DEG MT ABØVE MSL 945.00000 FT

Fig. 17 — Combined June 2, 10, 30 and July 30 data.

```
MØEGEN G3 - ØRØIT GENERATIØN ERØN ANOØVER TRAJECTØRIES  - L C THØNAS •

RANGE OATA SUPPLIEO ØN CENTRAL PØINT ØNLY.      FØRCEO FIT.

REFRACTIØN CØRRECTIØN APPLIED TØ INPUT ANO ØUTPUT SATELLITE ELEVATIØNS.

CØMPUTEO NØOIFIEO ØRBITAL ELEMENTS-

PØINT ITER      E P Ø C H          INCL    ASC  NØOE PSI 1OAY- ARG PERIG PERIGEE CHG ANØN PERIØO PERIØO CHG ECCEN-  RAO PERIGEE
 NØ    NØ  YEAR NØ OY HR MINUTE  OEGREES  WEST LØNG  NINUTES     OEG      OEG/TA       NIN      MIN/PERIØO TRICITY  STAT MILES

  1     4  1964  6 30  2 53.749  42.72775 219.27264  -0.12480 322.62804   0.19105   225.30049     0.       0.40134    4566.226
           1964  6 30  2 53.678           219.25497           322.62804   0.19115   225.41669 FRØM OATA PØINT 1 TØ 2 TIME
           1964  6 30  2 53.619           219.24006           322.62804   0.19123   225.51475 FRØM OATA PØINT 1 TØ 3 TIME
   ØRØIT ØFFSET =    31.49270 OEG ØF LAT.  IF O 1ST SUØSAT PØINT IN ØRBIT PLANE.


 (YEAR NØ OY HR NN SEC  (   PØINTING ANGLE CØNPARISØN - STATIØN AT ANOØVER NE   )
                        (   N-E-A-S-U-R-E-O          P-R-E-O-1-C-T-E-O     O  I  F  F  E  R  E  N  C  E  S  )
                         AZ-OEG EL-OEG RANGE-NI AZ-OEG EL-OEG RANGE-NI AZ-OIFF EL-OIFF ARC-OIF RANGE-OIFF)
 (1964  6 30  5 10 -0   210.36  37.45     0.   210.36  37.43  7449.74  -0.000    0.021   0.0221-7449.740 )
 (1964  6 30  5 20 -0   201.69  31.35  7347.55 201.67  31.31  7347.30   0.018    0.036   0.0400   0.251 )
 (1964  6 30  5 30 -0   193.71  23.77     0.   193.67  23.70  7211.21   0.039    0.070   0.0791-7211.212 )
 (1964  6 10  7 52 -0   280.67  27.72  8247.93 280.65  27.73  8259.59   0.016   -0.011   0.0185  -11.663 )
 (1964  6 10  0  0 -0   274.59  30.17  8101.17 274.58  30.17  8110.41   0.009   -0.003   0.0121   -9.237 )
 (1964  6 10  0 10 -0   266.01  32.14  7059.03 266.00  32.11  7065.60   0.010    0.027   0.0297   -5.853 )
 (1964  6  2  3 40 -0   275.88  25.01  6175.04 275.84  25.29  6193.00   0.041   -0.276   0.2783  -17.158 )
 (1964  6  2  3 42 -0   275.94  27.96  6186.80 275.90  28.22  6204.60   0.045   -0.259   0.2619  -17.801 )
 (1964  6  2  3 44 -0   275.97  30.03  6201.62 275.93  31.07  6219.99   0.040   -0.243   0.2458  -18.371 )
 (1964  6 30  5 10 -0   210.36  37.45  7446.59 210.36  37.43  7449.74  -0.000    0.021   0.0221   -3.150 )
 (1964  6 30  5 20 -0   201.69  31.35  7347.55 201.67  31.31  7347.30   0.018    0.036   0.0400    0.251 )
 (1964  6 30  5 30 -0   193.71  23.77  7214.50 193.67  23.70  7211.21   0.039    0.070   0.0791    3.288 )
 (1964  7 30 23 10 -0   287.17  15.74  4461.54 286.87  16.32  4467.66   0.297   -0.584   0.6496   -6.121 )
 (1964  7 30 23 20 -0   270.42  37.43  4523.02 270.05  37.02  4543.36   0.370   -0.387   0.4852  -19.539 )
 (1964  7 30 23 30 -0   246.88  49.01  4987.65 246.50  49.97  5012.97   0.378   -0.156   0.2896  -25.318 )
 (1964  8  1  1 50 -0   272.56  17.52  6562.70 272.38  17.68  6585.04   0.176   -0.159   0.2311  -22.340 )
 (1964  8  1  2  0 -0   260.38  21.80  7043.55 260.26  21.86  7066.20   0.119   -0.058   0.1249  -22.648 )
 (1964  8  1  2 10 -0   249.56  23.23  7537.26 249.49  23.25  7550.48   0.075   -0.023   0.0730  -21.223 )


AØØVE ELENENTS CØNPUTEO ERØN PØINTING ANGLES
FRØM ANOØVER ME   LAT   44.63550 OEG  WEST LØNG   70.70030 OEG  HT ABØVE NSL  945.00000 ET
```

Fig. 18 — Fit obtained with only one range point per determination: June 2, 10, 30 and July 30 data.

```
MØEGEN G3 - ØRBIT GENERATIØN FRØM ANDØVER TRAJECTØRIES  - L C THØMAS *

NØ RANGE DATA SUPPLIED TØ PRØGRAM FØR ØRBIT GENERATIØN   FØRCED FIT.

REFRACTIØN CØRRECTIØN APPLIED TØ INPUT AND ØUTPUT SATELLITE ELEVATIØNS.

CØMPUTED MØDIFIED ØRBITAL ELEMENTS-

PØINT ITER      E P Ø C H          INCL     ASC  NØDE PSI 1DAY- ARG PERIG PERIGEE CHG ANØM PERIØD PERIØD CHG ECCEN-  RAD PERIGEE
 NØ    NØ  YEAR MØ DY HR MINUTE  DEGREES  WEST LØNG  MINUTES     DEG      DEG/TA        MIN       MIN/PERIØD TRICITY  STAT MILES

 1     4  1964  6 30  2 53.023  42.68924 218.92101  -8.12480 321.70110  0.19105    225.30049     0.        0.39594    4608.807
          1964  6 30  2 50.623           218.31743           321.70110  0.19440    229.24918 FRØM DATA PØINT 1 TØ 2 TIME
          1964  6 30  2 50.597           218.31086           321.70110  0.19443    229.29213 FRØM DATA PØINT 1 TØ 3 TIME
   ØRBIT ØFFSET =    31.39869 DEG ØF LAT.  IF 0 1ST SUBSAT PØINT IN ØRBIT PLANE.


          (YEAR MØ DY HR MN SEC  (   PØINTING ANGLE CØMPARISØN - STATIØN AT ANDØVER ME   )
                                 (   M-E-A-S-U-R-E-D          P-R-E-D-I-C-T-E-D      D  I  F  F  E  R  E  N  C  E  S  I
                                 AZ-DEG EL-DEG RANGE-MI  AZ-DEG EL-DEG RANGE-MI AZ-DIFF EL-DIFF ARC-DIF RANGE-DIFFI
          (1964  6 30  5 10 -0   210.36  37.45      0.   210.36  37.43  7389.70  -0.000   0.021   0.0221-7389.703 I
          (1964  6 30  5 20 -0   201.69  31.35      0.   201.47  31.21  7284.01   0.224   0.138   0.2364-7284.007 )
          (1964  6 30  5 30 -0   193.71  23.77      0.   193.29  23.44  7149.13   0.423   0.329   0.5085-7149.133 )
          (1964  6  2  3 40 -0   275.88  25.01 6175.84  275.75  24.79  6246.59   0.134   0.218   0.2497  -70.748 )
          (1964  6  2  3 42 -0   275.94  27.96 6186.80  275.81  27.69  6255.35   0.133   0.271   0.2955  -68.549 )
          (1964  6  2  3 44 -0   275.97  30.83 6201.62  275.85  30.51  6267.71   0.123   0.318   0.3352  -66.089 )
          (1964  6 10  7 52 -0   280.67  27.72 8247.93  280.97  27.46  8233.58  -0.305   0.257   0.3728   14.352 )
          (1964  6 10  8  0 -0   274.59  30.17 8101.17  274.86  29.97  8073.53  -0.273   0.199   0.3092   27.637 )
          (1964  6 10  8 10 -0   266.01  32.14 7859.83  266.18  31.99  7816.45  -0.175   0.152   0.2123   43.376 )
          (1964  6 30  5 10 -0   210.36  37.45 7446.59  210.36  37.43  7389.70  -0.000   0.021   0.0221   56.887 )
          (1964  6 30  5 20 -0   201.69  31.35 7347.55  201.47  31.21  7284.01   0.224   0.138   0.2364   63.543 )
          (1964  6 30  5 30 -0   193.71  23.77 7214.50  193.29  23.44  7149.13   0.423   0.329   0.5085   65.367 )
          (1964  7 30 23 10 -0   287.17  15.74 4461.54  286.97  16.58  4530.10   0.202  -0.840   0.8617  -68.562 )
          (1964  7 30 23 20 -0   270.42  37.43 4523.82  270.62  37.67  4599.69  -0.195  -0.245   0.2896  -75.869 )
          (1964  7 30 23 30 -0   246.88  49.81 4987.65  247.63  49.86  5048.65  -0.750  -0.046   0.4864  -61.001 )
          (1964  8  1  1 50 -0   272.56  17.52 6562.70  272.99  17.61  6618.74  -0.434  -0.089   0.4235  -56.044 I
          (1964  8  1  2  0 -0   260.38  21.80 7043.55  260.94  21.83  7081.45  -0.560  -0.034   0.5212  -37.904 )
          (1964  8  1  2 10 -0   249.56  23.23 7537.26  250.15  23.30  7556.45  -0.586  -0.067   0.5423  -19.193 I


ABØVE ELEMENTS CØMPUTED FRØM PØINTING ANGLES
FRØM ANDØVER ME   LAT   44.63550 DEG  WEST LØNG   70.70030 DEG  HT ABØVE MSL  945.00000 FT
```

Fig. 19 — Same as Fig. 18, but with no range data.

TABLE II — ALTERATIONS TO MO ELEMENTS

Data Point of 4th Trajectory	Azimuth Alteration	Elevation Alteration	Range Alteration
1	0.21°	−0.07°	4.85 miles
2	0.06°	−0.02°	1.03 miles
3	−0.10°	+0.02°	−0.87 mile

from Andover data and used to simulate trajectories over Andover for a sequence of four passes. The computed pointing angles for these passes then were rounded off to the nearest hundredth of a degree so as to resemble typically reported data from Andover. Three points from each of the first 3 passes were then selected for submission to the MOEGEN G3 program. Three points from the fourth pass were purposely altered before submission to simulate the effects of tracking errors, mechanical jitter of the ground antenna, errors in assessment of refraction which affect measured position, and digital noise in the equipment at the ground station. These alterations were slight and are given in Table II. Using the data from the 4 passes, MOEGEN G3 produced 4 sets of orbital elements.

Fig. 20 displays the generated elements M1, M2, M3 and M4. For each of these elements, the first 3 lines of data under "pointing angle comparisons" (see Fig. 20) show the differences between the input data points of the submitted trajectories and those predicted by the derived elements. For each set of elements, the pointing error is within 0.07° and the range difference under 0.9 miles. Looking at each of the *first* 3 comparison lines, all 4 sets of elements produce excellent fits to reported Andover trajectories, and from this examination there would be no reason to expect that any particular set of elements would be decidedly better than any other. However, comparisons of the M4 orbit with 6/30 trajectory data indicate that something is wrong with these elements because of the increase in pointing angle differences on this date. This, however, could be produced by variety of causes: e.g., errors in epoch, rates, ellipse shape, size and orientation of the orbit. The point to make is that the M4 orbit fits well the trajectory over Andover from which it was derived; the purposely introduced errors in that trajectory have not done violence to the orbit theory, so that the motion of the satellite is in essential accord with those motions permitted by the earth's gravitational potential.

Using the same MO elements as previously, trajectories over Johannes-

```
MØEGEN G3 - ØR8IT GENERATIØN FRØM ANDØVER TRAJECTØRIES  - L C THØMAS *

3 PØINT RANGE DATA.     FIT FØRCED TØ AVERAGE RATES.

REFRACTIØN CØRRECTIØN APPLIED TØ INPUT AND ØUTPUT SATELLITE ELEVATIØNS.

CØMPUTED MØDIFIED ØRBITAL ELEMENTS-

PØINT ITER        E P Ø C H          INCL     ASC  NØDE PSI 1DAY- ARG PERIG PERIGEE CHG ANØM PERIØD PERIØD CHG ECCEN-  RAD PERIGEE
 NØ    NØ   YEAR MØ DY HR MINUTE   DEGREES  WEST LØNG  MINUTES     DEG      DEG/TA       MIN       MIN/PERIØD TRICITY  STAT MILES

 1     4   1964  6 30 17 55.214   42.74526  85.92082  -8.12480 323.58760   0.19105    225.30049     0.        0.40099    4564.555 MI
           1964  6 30 17 55.224             85.92345            323.58760   0.19094    225.17527 FRØM DATA PØINT 1 TØ 2 TIME
           1964  6 30 17 55.228             85.9243D            323.58760   0.19091    225.13461 FRØM DATA PØINT 1 TØ 3 TIME
    ØRBIT ØFFSET =    24.26940 DEG ØF LAT.  (F 0 1ST SUBSAT PØINT IN ØRBIT PLANE.


          (YEAR MØ DY HR MN SEC  (   PØINTING ANGLE CØMPARISØN - STATIØN AT ANDØVER ME   I
                                 (   M-E-A-S-U-R-E-D          P-R-E-D-I-C-T-E-D    D I F F  E R R E N C E S  )
                                 AZ-DEG EL-DEG RANGE-MI AZ-DEG EL-DEG RANGE-MI AZ-DIFF EL-DIFF ARC-DIFF RANGE-DIFF)
          (1964  6 30 18 14 -0   172.10  25.01  2526.48 172.10  24.98  2526.48  -0.000   0.035   0.0363    0.004 )
          (1964  6 30 18 24 -0   113.28  41.45  3089.51 113.29  41.43  3089.32  -0.007   0.017   0.0221    0.186 )
          (1964  6 30 18 34 -0    82.95  32.12  4435.73  82.96  32.10  4435.08  -0.005   0.019   0.0221    0.652 )
          (1964  6 30 18 14 -0   172.10  25.01  2526.48 172.10  24.98  2526.48  -0.000   0.035   0.0363    0.004 )
          (1964  6 30 18 24 -0   113.28  41.45  3089.51 113.29  41.43  3089.32  -0.007   0.017   0.0221    0.186 )
          (1964  6 30 18 34 -0    82.95  32.12  4435.73  82.96  32.10  4435.08  -0.005   0.019   0.0221    0.652 )
          (1964  6 30 22 20 -0   253.31  67.71  3592.57 253.32  67.69  3592.28  -0.005   0.024   0.0262    0.291 )
          (1964  6 30 22 30 -0   134.39  85.02  4284.55 134.52  85.02  4283.77  -0.129  -0.005   0.0140    0.775 )
          (1964  6 30 22 40 -0    96.87  69.49  5133.89  96.88  69.49  5132.73  -0.010  -0.005   0.0140    1.162 )
          (1964  7  1  2 30 -0   275.16  46.86  5950.66 275.16  46.85  5949.91  -0.003   0.009   0.0140    0.754 )
          (1964  7  1  2 40 -0   262.01  56.52  6228.15 262.02  56.49  6227.08  -0.014   0.027   0.0297    1.071 )
          (1964  7  1  2 50 -0   243.63  62.12  6516.14 243.65  62.10  6514.79  -0.023   0.020   0.0252    1.348 )
          (1964  7  1  6 50 -0   278.01  14.41  8863.39 278.01  14.40  8862.02  -0.004   0.007   0.0121    1.367 )
          (1964  7  1  7  0 -0   270.85  15.34  8919.85 270.85  15.34  8918.32  -0.003   0.004   0.0121    1.530 )
          (1964  7  1  7 10 -0   263.66  15.23  8909.19 263.66  15.16  8907.54  -0.004   0.065   0.0660    1.647 )
```

Fig. 20 — Modified orbital elements generated from simulated Andover passages.

PØINT NØ	ITER NØ	EPØCH YEAR	MØ	DY	HR	MINUTE	INCL DEGREES	ASC NØDE WEST LØNG	PSI 10AY-MINUTES	ARG PERIG DEG	PERIGEE CHG DEG/TA	ANØM MIN	PERIØD MIN/PERIØD	PERIØD CHG ECCENTRICITY	RAØ PERIGEE STAT MILES	
1	4	1964	6	30	21	40.503	42.74677	142.55847	-8.12480	323.75162	0.19105	225.30049	0.	0.40110	4563.160	M2
		1964	6	30	21	40.543		142.56851		323.75162	0.19086	225.07273	FRØM DATA PØINT 1 TØ 2 TIME			
		1964	6	30	21	40.552		142.57085		323.75162	0.19081	225.01965	FRØM DATA RØINT 1 TØ 3 TIME			
ØRBIT ØFFSET = 3.77641 DEG ØF LAT. IF 0 1ST SUBSAT PØINT IN ØRBIT PLANE.																

IYEAR	MØ	DY	HR	MN	SEC	RØINTING ANGLE CØMPARISØN – STATIØN AT ANDØVER ME: M-E-A-S-U-R-E-D AZ-DEG	EL-DEG	RANGE-MI	P-R-E-D-I-C-T-E-D AZ-DEG	EL-DEG	RANGE-MI	D I F F E R E N C E S AZ-DIFF	EL-DIFF	ARC-DIF	RANGE-DIFF
I1964	6	30	22	20	-0	253.31	67.71	3592.57	253.31	67.70	3592.56	0.000	0.007	0.0140	0.010
I1964	6	30	22	30	-0	134.39	85.02	4284.55	134.46	85.02	4284.26	-0.070	-0.004	0.0156	0.291
I1964	6	30	22	40	-0	96.87	69.49	5133.89	96.87	69.50	5133.07	-0.002	-0.009	0.0156	0.822
I1964	6	30	18	14	-0	172.10	25.01	2526.48	172.05	24.99	2525.78	0.051	0.015	0.0490	0.703
I1964	6	30	18	24	-0	113.28	41.45	3089.51	113.25	41.42	3090.01	0.032	0.026	0.0370	-0.504
I1964	6	30	18	34	-0	82.95	32.12	4435.73	82.94	32.09	4435.89	0.006	0.026	0.0280	-0.164
I1964	6	30	22	20	-0	253.31	67.71	3592.57	253.31	67.70	3592.56	0.000	0.007	0.0140	0.010
I1964	6	30	22	30	-0	134.39	85.02	4284.55	134.46	85.02	4284.26	-0.070	-0.004	0.0156	0.291
I1964	6	30	22	40	-0	96.87	69.49	5133.89	96.87	69.50	5133.07	-0.002	-0.009	0.0156	0.822
I1964	7	1	2	30	-0	275.16	46.86	5950.66	275.17	46.85	5950.34	-0.011	0.011	0.0156	0.322
I1964	7	1	2	40	-0	262.01	56.52	6228.15	262.04	56.49	6227.42	-0.033	0.031	0.0370	0.731
I1964	7	1	2	50	-0	243.63	62.12	6516.14	243.69	62.10	6514.94	-0.055	0.022	0.0357	1.200
I1964	7	1	6	50	-0	278.01	14.41	8863.39	278.03	14.40	8862.05	-0.021	0.009	0.0210	1.340
I1964	7	1	7	0	-0	270.85	15.34	8919.85	270.87	15.33	8918.16	-0.022	0.006	0.0221	1.689
I1964	7	1	7	10	-0	263.66	15.23	8909.19	263.68	15.16	8907.18	-0.024	0.066	0.0699	2.011

PØINT NØ	ITER NØ	EPØCH YEAR	MØ	DY	HR	MINUTE	INCL DEGREES	ASC NØDE WEST LØNG	PSI 10AY-MINUTES	ARG PERIG DEG	RERIGEE CHG DEG/TA	ANØM MIN	PERIØD MIN/RERIØD	PERIØD CHG TRICITY	ECCEN-	RAØ PERIGEE STAT MILES	
1	4	1964	7	1	1	25.832	42.74387	199.19972	-8.12480	323.98413	0.19105	225.30049	0.	0.40093		4566.160	M3
		1964	7	1	1	25.913		199.22009		323.98413	0.19081	225.01610	FRØM DATA PØINT 1 TØ 2 TIME				
		1964	7	1	1	25.897		199.21608		323.98413	0.19086	225.07210	FRØM DATA PØINT 1 TØ 3 TIME				
ØRBIT ØFFSET = 3.29539 DEG ØF LAT. IF 0 1ST SUBSAT RØINT IN ØRBIT PLANE.																	

IYEAR	MØ	DY	HR	MN	SEC	RØINTING ANGLE CØMPARISØN – STATIØN AT ANDØVER ME: M-E-A-S-U-R-E-D AZ-DEG	EL-DEG	RANGE-MI	P-R-E-D-I-C-T-E-D AZ-DEG	EL-DEG	RANGE-MI	D I F F E R E N C E S AZ-DIFF	EL-DIFF	ARC-DIF	RANGE-DIFF
I1964	7	1	2	30	-0	275.16	46.86	5950.66	275.16	46.86	5950.65	-0.000	0.000	0.0121	0.009
I1964	7	1	2	40	-0	262.01	56.52	6228.15	262.02	56.51	6228.07	-0.006	0.014	0.0185	0.079
I1964	7	1	2	50	-0	243.63	62.12	6516.14	243.63	62.11	6516.09	-0.002	0.006	0.0121	0.054
I1964	6	30	18	14	-0	172.10	25.01	2526.48	172.15	24.94	2528.07	-0.049	0.074	0.0865	-1.593
I1964	6	30	18	24	-0	113.28	41.45	3089.51	113.34	41.43	3089.31	-0.061	0.016	0.0490	0.198
I1964	6	30	18	34	-0	82.95	32.12	4435.73	82.97	32.11	4435.01	-0.023	0.012	0.0221	0.719
I1964	6	30	22	20	-0	253.31	67.71	3592.57	253.30	67.67	3592.73	0.008	0.042	0.0431	-0.162
I1964	6	30	22	30	-0	134.39	85.02	4284.55	134.58	85.02	4284.29	-0.190	-0.005	0.0198	0.265
I1964	6	30	22	40	-0	96.87	69.49	5133.89	96.88	69.49	5133.60	-0.007	-0.002	0.0121	0.292
I1964	7	1	2	30	-0	275.16	46.86	5950.66	275.16	46.86	5950.65	-0.000	0.000	0.0121	0.009
I1964	7	1	2	40	-0	262.01	56.52	6228.15	262.02	56.51	6228.07	-0.006	0.014	0.0185	0.079
I1964	7	1	2	50	-0	243.63	62.12	6516.14	243.63	62.11	6516.09	-0.002	0.006	0.0121	0.054
I1964	7	1	6	50	-0	278.01	14.41	8863.39	278.00	14.42	8863.19	0.006	-0.009	0.0140	0.203
I1964	7	1	7	0	-0	270.85	15.34	8919.85	270.84	15.35	8919.67	0.009	-0.012	0.0140	0.179
I1964	7	1	7	10	-0	263.66	15.23	8909.19	263.65	15.18	8909.08	0.010	0.048	0.0504	0.113

Fig. 20 (cont.).

```
POINT ITER      E P O C H          INCL     ASC  NODE PSI 10AY- ARG PERIG PERIGEE CHG AMOM PERIOD PERIOD CHG ECCEN-  RAD PERIGEE
 NO    NO   YEAR MO DY HR MINUTE  DEGREES  WEST LONG  MINUTES     DEG      DEG/TA      MIN      MIN/PERIOD TRICITY  STAT MILES

 1     4   1964  7  1  5 11.133  42.72288 255.82689  -8.12480 324.12966   0.19105   225.30049     0.       0.41158   4450.926 M4
           1964  7  1  5 11.481           255.91451           324.12966   0.19038   224.50626 FROM DATA POINT 1 TO 2 TIME
           1964  7  1  5 11.473           255.91253           324.12966   0.19039   224.52418 FROM DATA POINT 1 TO 3 TIME
     ORBIT OFFSET =   15.26678 DEG OF LAT.  IF 0 1ST SUBSAT POINT IN ORBIT PLANE.

          (YEAR MO DY HR MN SEC  (   POINTING ANGLE COMPARISON - STATION AT AMOVER ME   )
                                 (   M-E-A-S-U-R-E-D          P-R-E-D-I-C-T-E-D      D  I  F  F  E  R  E  N  C  E  S  )
                                 AZ-DEG EL-DEG RANGE-MI AZ-DEG EL-DEG RANGE-MI AZ-DIFF EL-DIFF ARC-DIF RANGE-DIFF)
          (1964  7  1  6 50 -0   277.80  14.48  8858.54 277.80  14.48  8858.54  -0.000   0.000   0.0121    0.004 )
          (1964  7  1  7  0 -0   270.79  15.36  8918.82 270.81  15.35  8919.04  -0.021   0.006   0.0185   -0.215 )
          (1964  7  1  7 10 -0   263.76  15.21  8910.06 263.80  15.15  8910.24  -0.043   0.056   0.0699   -0.182 )
          (1964  6 30 18 14 -0   172.10  25.01  2526.48 169.14  25.05  2428.05   2.955  -0.041   2.6780   98.428 )
          (1964  6 30 18 24 -0   113.28  41.45  3089.51 109.84  39.88  3081.05   3.438   1.566   3.0420    8.459 )
          (1964  6 30 18 34 -0    82.95  32.12  4435.73  81.56  30.45  4469.52   1.390   1.668   2.0475  -33.787 )
          (1964  6 30 22 20 -0   253.31  67.71  3592.57 251.68  70.04  3535.27   1.635  -2.328   2.4012   57.299 )
          (1964  6 30 22 30 -0   134.39  85.02  4284.55 121.53  83.50  4272.76  12.860   1.522   1.9842   11.789 )
          (1964  6 30 22 40 -0    96.87  69.49  5133.89  96.34  68.05  5144.37   0.535   1.444   1.4571  -10.484 )
          (1964  7  1  2 30 -0   275.16  46.86  5950.66 274.19  47.76  5913.86   0.965  -0.904   1.1151   36.801 )
          (1964  7  1  2 40 -0   262.01  56.52  6228.15 260.79  57.08  6209.12   1.216  -0.564   0.8727   19.030 )
          (1964  7  1  2 50 -0   243.63  62.12  6516.14 242.38  62.35  6508.58   1.255  -0.233   0.6293    7.562 )
          (1964  7  1  6 50 -0   278.01  14.41  8863.39 277.80  14.48  8858.54   0.210  -0.070   0.2149    4.854 )
          (1964  7  1  7  0 -0   270.85  15.34  8919.85 270.81  15.35  8919.04   0.039  -0.014   0.0402    0.815 )
          (1964  7  1  7 10 -0   263.66  15.23  8909.19 263.80  15.15  8910.24  -0.143   0.076   0.1581   -1.052 )
```

Fig. 20 (cont.).

burg, South Africa were produced. These were compared with the predictions from the generated M4 elements in a computer comparison program. The results are given in Fig. 21, where all listed data are for satellite positions not visible to Andover (subsatellite latitudes 4° to −42°). The average pointing error is 2.7° and the root-mean-square range error is 65.5 miles.

The four generated elements were then submitted to the MOEFIT program, which applies the principles of Section VIII to generate an ellipse of best fit using only those portions of the orbits, described by the input elements, which are visible from Andover. Fig. 22 shows the eccentricity of 0.400593 and the perigee radius of 4565.168 statute miles determined from this ellipse. It also indicates that the root-mean-square departure of the fitted ellipse from those points generated by the four elements is in the order of 10^{-7}. Fig. 23 graphs the fitted ellipse as a curved line, while the points visible from Andover and predicted by the individual elements are noted by zeros on the plot.

The M4 set of elements was then altered by substituting the eccentricity and radius of perigee values from the MOEFIT program and was again compared with Johannesburg trajectories given by the original set of elements, MO. Typical results are given in Fig. 24, where it is seen that the average pointing angle error is now 0.07°, about 2 orders

```
@EUNO-THE-W@RLO-@R817-7ES1  - M@ES GENERATED FN AND@VER   L C 7H@MAS

@R817AL ELEMENTS M-4 F@@M M@EGEN G3 USED.

SIATI@N AT J@@URG, S.AF LAT= -26.03246 OEG   WEST L@NG =  331.75878 OEG  HT A@@VE NSL= 5370.00000 FT

YEAR N@ DY HR MN SEC     SAT P@S FR@M  M@E 1      SAT P@S FR@M  OATA      D I F F E R E N C E S
                      AZ-DEG EL-OEG RANGE-NI AZ-DEG EL-OEG RANGE-MI AZ-DIFF EL-DIFF ARC-DIF RANGE-DIFF
1964  6 30  1 50  0   288.75  11.10  7605.79 288.53  11.98  7559.01  -0.221   0.878   0.9043   -46.777
1964  6 30  2  0  0   284.15  18.01  6463.13 283.78  19.20  6411.44  -0.367   1.191   1.2407   -51.693
1964  6 30  2 10  0   277.26  26.86  5135.54 276.55  28.50  5085.55  -0.713   1.635   1.7529   -49.993
1964  6 30  2 20  0   263.52  39.54  3647.60 261.69  41.83  3616.87  -1.829   2.287   2.6741   -30.732
1964  6 30  2 30  0   213.29  54.33  2253.39 206.47  55.47  2295.77  -6.816   1.137   4.0786    42.382
1964  6 30  2 40  0   136.40  14.84  2296.01 134.91  14.78  2430.20  -1.487  -0.057   1.4384   134.186
1964  7  1  4 40  0   251.49   2.50  5127.70 250.75   4.33  5068.46  -0.737   1.834   1.9758   -59.242
1964  7  1  4 50  0   236.65  14.72  3173.39 235.10  17.25  3136.97  -1.549   2.525   2.9315   -36.423
1964  7  1  5  0  0   174.13  27.48  1518.65 169.84  29.93  1586.01  -4.293   2.448   4.4906    67.362
1964  7  1  8 56  0   277.23  31.34   832.02 277.78  37.04   906.03   0.549   5.697   5.7154    74.006

M@DIFIED @@BITAL ELEMENTS F@R A@@VE TABLE ARE-                          AVG=2.7202   65.541=RMS

 ELEMENTS N@   1
@EFERENCE TIME 1964  7  1   5 HR 11.13300 MIN UT
INCLINATI@N  42.72288 OEG
ASCENDING N@DE WEST L@NG 255.82689 OEG
P@INE SWEEP IN7E@VAL = 1 DAY -8.124800 MIN
PERIGEE AND SATELLITE ARGUMENT 324.12966 OEG
    RATE @F CHANGE  0.191050 OEG PER PER180
ANOMALISTIC PERI@D  225.30049 MIN
    RATE @F CHANGE@.          MIN PER PER180
ECCENTRICITY 0.4115810
@ADIUS @F PE@IGEE  4450.926 STATUTE MILES
```

Fig. 21 — Comparison of M4 elements to Johannesburg trajectories derived from MO.

```
RØUND-THE-WØRLD-ØRBIT-TEST  - MØES GENERATED FM ANDØVER   L C THØMAS
 SUCCESSIØN ØF PASSES ØN 6/30 AND 7/1/1964 USED FØR RP,E DETERMINATIØN
                                    ABS VALUE ØF MAX ERRØR=  5.8822479E-07
LEAST SQUARES ØRBITAL ELEMENT VALUES- MEAN SQUARE ERRØR=  2.1384752E-14
                                    RMS ERRØR=  1.4623526E-07
ECCENTRICITY =   0.4DD593 RADIUS ØE PERIGEE =  4565.1683 STATUTE MILES
SEMI-MAJØR AXIS =   7616.1472 STATUTE MILES

    AVERAGE PERIGEE PØSITIØN =  324.14983 DEG AT EPØCH ØE FIRST MØES

INPUT MØDIFIED ØRBITAL LIST EØLLØWS-

REFERENCE TIME 1964  6 3D 17 HØUR 55.214DD MIN U.T.
INCLINATIØN   42.74526 DEG
ASCENDING NØDE LØNG   85.92082DEG WEST
PRIME SWEEP INTERVAL ØNE DAY   -8.1248D MIN
PERIGEE AND SATELLITE PØSITIØN  323.5876D DEG
    RATE ØF CHANGE   0.19105 DEG PER PERIØD
ANØMALISTIC PERIØD  225.3DD49 MIN
    RATE ØF CHANGE    D.       MIN PER PERIØD
ECCENTRICITY    0.40099
RADIUS ØF PERIGEE  4564.55493 STATUTE MILES

START CARD IMAGE IS-
1964  6 3D 16  7  0     70  6D  60

REFERENCE TIME 1964  6 30 21 HØUR 40.5D3ØD MIN U.T.
INCLINATIØN   42.74677 DEG
ASCENDING NØDE LØNG  142.55847DEG WEST
PRIME SWEEP INTERVAL ØNE DAY   -8.1248D MIN
PERIGEE AND SATELLITE PØSITIØN  323.75162 DEG
    RATE ØF CHANGE   0.19105 DEG PER PERIØD
ANØMALISTIC PERIØD  225.3DD49 MIN
    RATE ØE CHANGE    0.       MIN PER PERIØD
ECCENTRICITY    0.4D1T0
RADIUS ØF PERIGEE  4563.15997 STATUTE MILES

START CARD IMAGE IS-
1964  6 30 22  1  D     124 12D 120

REEERENCE TIME 1964  7  1  1 HØUR 25.832DD MIN U.T.
INCLINATIØN   42.74387 DEG
ASCENDING NØDE LØNG  199.19972DEG WEST
PRIME SWEEP INTERVAL ØNE DAY   -8.12480 MIN
PERIGEE AND SATELLITE PØSITIØN  323.98413 DEG
    RATE ØE CHANGE   0.19105 DEG PER PERIØD
ANØMALISTIC PERIØD  225.3DD49 MIN
    RATE ØF CHANGE    D.       MIN PER PERIØD
ECCENTRICITY    0.40093
RADIUS ØE PERIGEE  4566.15997 STATUTE MILES

START CARD IMAGE IS-
1964  7  1  2  2  0     138 120 120

REFERENCE TIME 1964  7  1  5 HØUR 11.133DD MIN U.T.
INCLINATIØN   42.72288 DEG
ASCENDING NØDE LØNG  255.826890EG WEST
PRIME SWEEP INTERVAL ØNE DAY   -8.12480 MIN
PERIGEE ANO SATELLITE PØSITIØN  324.12966 DEG
    RATE ØE CHANGE   0.19105 DEG PER PERIØD
ANØMALISTIC PERIØD  225.3DD49 MIN
    RATE ØF CHANGE    D.       MIN PER PERIØD
ECCENTRICITY    D.41158
RADIUS ØE PERIGEE  4450.92596 STATUTE MILES

START CARD IMAGE IS-
1964  7  1  6 14  D     99  6Q  60
```

M1

M2

M3

M4

Fig. 22 — Eccentricity and perigee radius from ellipse of least-squares fit.

of magnitude better than the value before ellipse fitting. The root-mean-square range error has decreased an order of magnitude and is now 5.2 statute miles.

It is to be noted that only four passes at Andover were used in this illustrative procedure, since these four encompassed the entire portion of the orbit visible from Andover. However, as apsidal advance takes place,

new portions of the orbit become visible and, provided little orbit decay occurs, these may also be used to obtain even better ellipse fits and further refine values for the eccentricity and perigee radius.

It is also noted that in actual practice each of the trajectories used would have suffered slight measurement errors akin to those artificially introduced into the fourth trajectory that produced elements M4. Nonetheless, the derived elements would predict well that portion of the orbit ellipse from which they came (as was demonstrated by M4) and would therefore be improved by MOEFIT for round-the-world use by about the same amounts as shown in the illustrated example.

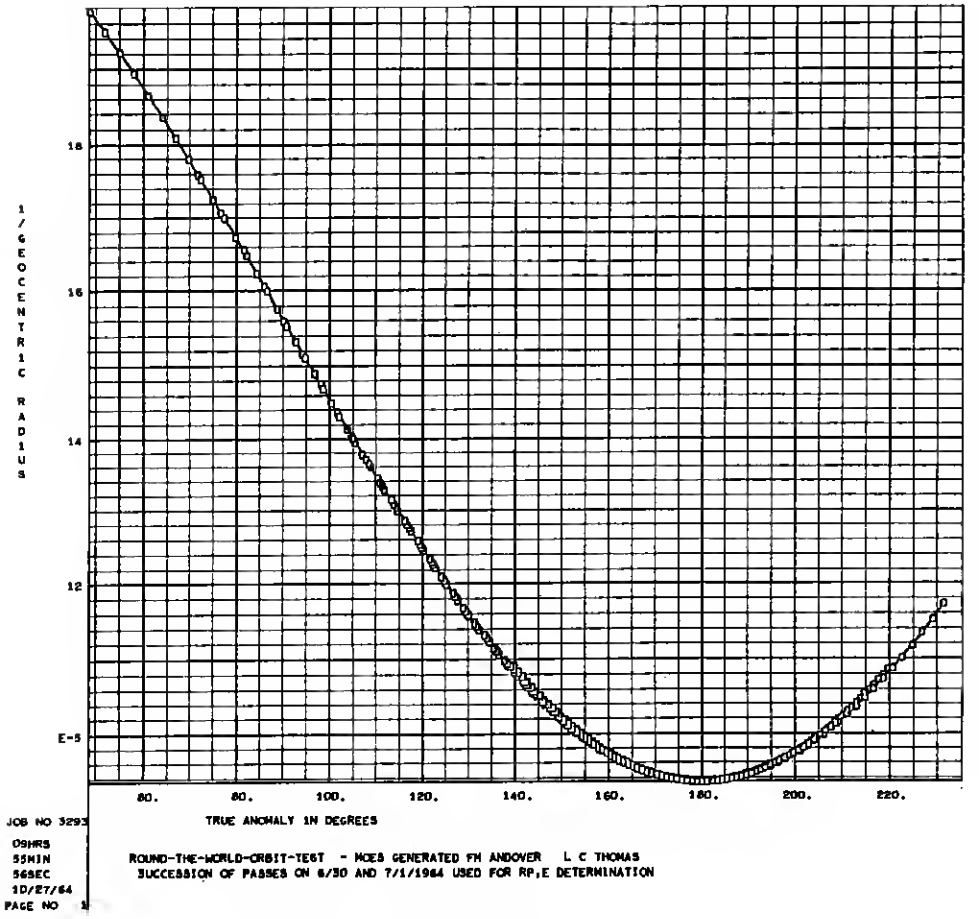

Fig. 23 — Ellipse of least-squares fit to elements.

XII. CONCLUSIONS

The methods described have been used extensively for those orbit determinations of the TELSTAR satellites dealing with the satellite communications experiment. The following merits of this orbital technique are noted:

(*i*) The elements chosen explicitly express the secular rates, thereby simplifying and making more economical the generation of predicted trajectories and drive tapes for the Andover antenna.

(*ii*) The generation procedure is geared to sparse and discontinuous tracking data.

(*iii*) Using a modified Gaussian technique for orbit generation provides a straightforward method for range determination to which orbital perturbations are easily added on an iterative basis.

(*iv*) The computation of secular rates only saves time and money and proves adequate for the tracking requirements of the TELSTAR satellite experiments (0.05° pointing accuracy).

(*v*) For cases where the secular rates are not constant over a given span of time, the methods described will still function provided tracking data are available frequently enough to assure essentially constant rates from each data acquisition time to the next.

(*vi*) The method provides for the operational inclusion of perturbations

```
RØUND-THE-WØRLD-ØRBIT-TEST  -  MØES GENERATED FM ANDØVER   L C THØMAS

M-4 ELEMENTS WITH ECCENTRICITY AND RADIUS ØF PERIGEE FRØM MØEFIL.

STATIØN AT JØHBURG, S.AF LAT=  -26.03246 DEG   WEST LØNG =  331.75878 DEG  NT AØØVE MSL= 5370.00000 FT

YEAR MØ DY HR MN SEC     SAT PØS FRØM  MØE 1      SAT PØS FRØM  DATA     D I F F E R E N C E S
                         AZ-DEG EL-DEG RANGE-MI AZ-DEG EL-DEG RANGE-MI AZ-DIFF EL-DIFF ARC-DIF RANGE-DIFF
1964  6 30  1 50  0     288.56  11.97  7550.87 288.53  11.98  7559.01  -0.027   0.009   0.02R0    R.142
1964  6 30  2  0  0     283.81  19.20  6403.74 283.7R  19.20  6411.44  -0.027   0.003   0.0242    7.704
1964  6 30  2 10  0     276.59  28.51  5078.57 276.55  2R.50  50R5.55  -0.040  -0.007   0.0370    6.983
1964  6 30  2 20  0     261.72  41.85  3611.05 261.69  41.R3  3616.R7  -0.034  -0.017   0.0321    5.R21
1964  6 30  2 30  0     206.38  55.52  2292.20 206.47  55.47  2295.77   0.091  -0.047   0.0699    3.566
1964  6 30  2 40  0     134.85  14.72  2429.9R 134.9I  14.7R  243D.20   0.055   0.064   0.DR33    0.222
1964  7  1  4 40  0     250.7R   4.16  5062.97 25D.75   4.33  5068.46  -0.029   0.16R   0.1700    5.492
1964  7  1  4 50  0     235.13  17.22  3133.32 235.10  17.25  3136.97  -0.026   0.026   0.0350    3.653
1964  7  1  5  0  0     169.84  29.94  1584.84 169.R4  29.93  1586.01   0.000  -0.012   0.0171    I.166
1964  7  1  8 56  0     277.52  36.95   90R.26 277.78  37.04   906.03   0.264   0.093   0.2305   -2.234
                                                                                    AVG=0.0727   5.209=RMS

MØDIFIED ØRBITAL ELEMENTS FØR ANØVE TABLE ARE-

 ELEMENTS MØ   1
REFERENCE TIME 1964  7  1    5 HR 11.13300 MIN UT
INCLINATIØN  42.722RR DEG
ASCENDING MØDE WEST LØNG 255.82689 DEG
PRIME SWEEP INTERVAL = 1 DAY -R.124800 MIN
PERIGEE AND SATELLITE ARGUMENT 324.12966 DEG
    RATE ØF CHANGE  0.191050 DEG PER PERIØD
ANØMALISTIC PERIØD  225.30049 MIN
    RATE ØF CHANGE0.            MIN PER PERIØD
ECCENTRICITY D.4005930
RADIUS ØF PERIGEE  4565.168 STATUTE MILES
```

M4 - MODIFIED

Fig. 24 — Comparison of M4 elements (with fitted ellipse corrections) to Johannesburg trajectories.

not computed here. For example, cyclic perturbations may be expressed, if indicated in the data, by generation of a multiplicity of elements over a time span and noting the derivatives of the "secular" rates.

XIII. ACKNOWLEDGMENTS

The author gratefully acknowledges his indebtedness to all those authors listed in the references, particularly those greats of the past — such as Gauss and LaPlace — who, under less favorable conditions, produced the earlier "breakthroughs" from which the lesser of us now derive benefit.

APPENDIX A

Relationship of the Triangular Area between Two Radius Vectors and the Orbit Normal

Consider triangle 023 of Fig. 4 and project it upon the yz plane. The vertices of the projected triangle are, therefore, (0,0,0), $(0,y_3,z_3)$, $(0,y_2,z_2)$ and hence its area becomes

$$A_p = \tfrac{1}{2}(y_2z_3 - z_2y_3). \tag{119}$$ *

Now the normal to the yz plane is, of course, the x axis. The normal to the orbit plane, shown in Fig. 4, makes an angle n with the x axis. Since the area of triangle 023 is the projected area referred to above divided by the cosine of the angle between the orbit plane and the yz plane, and since this angle is the same as the angle n between the normals to the two planes, it follows directly that the area of 023 is

$$A_{023} = \tfrac{1}{2}(y_2z_3 - z_2y_3)/\cos n \tag{120}$$

or

$$y_2z_3 - z_2y_3 = A_{23}\cos n \tag{9}$$

where

$$A_{23} = 2A_{023}\,. \tag{121}$$

APPENDIX B

Relations Involving the Earth's Oblateness

Because the earth is not a perfect sphere, two corrections are normally applied to satellite positional data as measured from any specified ground

* See page 266, Ref. 23.

station. The same corrections in the inverse sense are applied when trajectory predictions are made from orbital elements. The first of these recognizes that the geocentric distance of the station is a function of geodetic latitude; the second correction relates to the change in azimuth and elevation of the satellite when referred to a spherical as opposed to an oblate earth.

The geocentric distance[5] of the station is simply

$$R = H + R_E(0.998320047 + 0.001683494 \cos 2\varphi - 0.000003549 \cos 4\varphi + 0.000000008 \cos 6\varphi) \tag{125}$$

where

H = the height of the station above mean sea level in statute miles
R_E = the earth's equatorial radius = 3963.347 statute miles
φ = the geodetic latitude of the station.

This indicated value of R is used in solving for the satellite's slant range as in Section IV of the text. It is also used to determine the X_i, Y_i, Z_i station coordinates in Section 5.3.

Normally, azimuth-elevation measurements of a satellite made from a ground station are based upon measurements referenced to a local horizontal plane. This plane is often taken as a tangent to the oblate earth at the station's location. It becomes useful to reference such azimuth-elevation measurements to a plane tangent at the station to a sphere having a radius R. This is done both in trajectory prediction (Section IV) and in preprocessing the azimuth-elevation data prior to orbit determinations.

To relate the azimuth-elevation points to the two tangent planes, we begin by establishing two right-hand coordinate systems, centered on the station. In the first of these, the x-y axes lie in the plane tangent to the oblate earth with the y axis pointing northward and the x axis eastward. In the second system, the x-y' axes lie in the plane tangent to a sphere of radius R. The transformation from one system to the other is a simple one, since rotation of the first set of coordinates about the common x axis moves y into y' as shown in Fig. 25(a).

By inspection of Fig. 25(b), we write the measured azimuth (A) and elevation (E) in terms of the xyz coordinates (referenced to the oblate earth) as

$$x = \rho \cos E \sin A \tag{126}$$

$$y = \rho \cos E \cos A \tag{127}$$

$$z = \rho \sin E \tag{128}$$

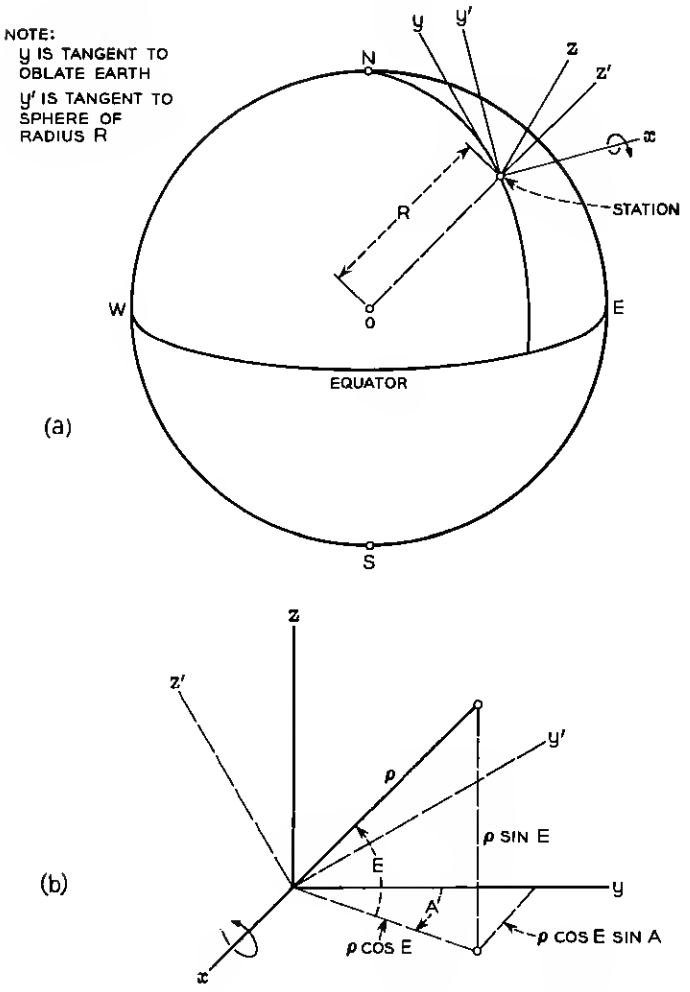

Fig. 25 — Geometry for correcting earth oblateness effects.

where

$$\rho = \text{the slant range to the satellite.}$$

Next we rotate the xyz coordinates about x through an angle $(\alpha)^*$ equal to the difference between the geodetic and geocentric latitude of the station. This brings y into y' and z into z' where $xy'z'$ is the coordinate

* α = geocentric latitude − geodetic latitude $\approx$ 0.1962 sin (geodetic latitude). A closer approximation is found in Ref. 5.

system for a sphere of radius R. The relationships between y,y' and z,z' are

$$y' = y \cos \alpha + z \sin \alpha \tag{129}$$

$$z' = -y \sin \alpha + z \cos \alpha. \tag{130}$$

Combining (126) through (130) one obtains

$$x = \rho \cos E \sin A \tag{131}$$

$$y' = \rho \cos E \cos A \cos \alpha + \rho \sin E \sin \alpha \tag{132}$$

$$z' = -\rho \cos E \cos A \sin \alpha + \rho \sin E \cos \alpha \tag{133}$$

from which the azimuth (A') and elevation (E') referred to the sphere become

$$E' = \sin^{-1} z'/\rho \tag{134}$$

$$A' = \tan^{-1} x/y'. \tag{135}$$

The procedure is perfectly symmetrical, and if one wants to convert from spherically oriented azimuth-elevation to the oblate earth azimuth-elevation, (131) through (135) are used with a negative α and interchanged primes.

APPENDIX C

The Triangle Ratios m_1 and m_3 as Time Functions

Consider the orbit ellipse lying in the xy plane as shown in Fig. 26. The observed positions of the satellite are expressed in x,y coordinates and time t. If we now define a new time variable $\tau = kt$, the familiar differential equations of motion then become

$$\frac{d^2x}{d\tau^2} = -k^2 \frac{x}{r^3} \tag{138}$$

and

$$\frac{d^2y}{d\tau^2} = -k^2 \frac{y}{r^3}. \tag{139}$$

Considering points 1 and 2, we may expand x_1 and y_1 in a Taylor series which generally converges for all reasonable values of τ:

$$x_1 = x_2 + \frac{dx}{d\tau} \tau_3 + \frac{1}{2!} \frac{d^2x}{d\tau^2} \tau_3^2 + \cdots \tag{140}$$

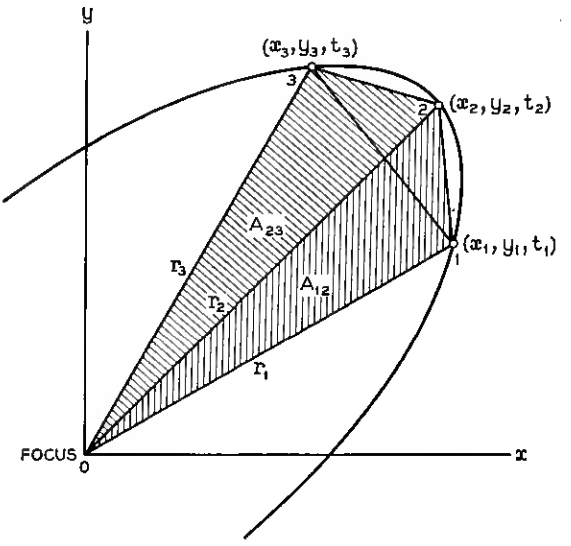

Fig. 26 — Orbit triangles in x,y,t space.

$$y_1 = y_2 + \frac{dy}{d\tau}\tau_3 + \frac{1}{2!}\frac{d^2y}{d\tau^2}\tau_3^2 + \cdots \tag{141}$$

where the τ derivatives are to be evaluated at the time t_2 of the second data point. We define τ_3 in the text. Similar expressions may of course be written for points 2 and 3. It is possible to substitute for all the derivatives in (140) and (141) higher than the first by successive differentiation of (138) and (139). This permits (140) and (141) to be expressed as

$$x_1 = A_1 x_2 + B_1 \frac{dx}{d\tau} \tag{142}$$

$$y_1 = A_1 y_2 + B_1 \frac{dy}{d\tau} \tag{143}$$

where

$$A_1 = 1 - \frac{1}{2}\left(\frac{\tau_3^2}{r_2^3} + \frac{\tau_3^3}{r_2^4}\frac{dr}{d\tau}\right) + \cdots \tag{144}$$

$$B_1 = \tau_3 - \frac{\tau_3^2}{6r_2^3} + \frac{\tau_3^4}{4r_2^4}\frac{dr}{d\tau} + \cdots. \tag{145}$$

Point x_3, y_3 may be expressed in a manner identical to (142)–(145) with subscript 1 being replaced by 3 throughout and τ_3 becoming τ_2.

The areas of the triangles formed by r_1, r_2, and r_3 and their respective chords are[23]

$$A_{12} = \tfrac{1}{2}(x_1y_2 - y_1x_2) \tag{146}$$

and

$$A_{23} = \tfrac{1}{2}(x_2y_3 - y_2x_3). \tag{147}$$

If now (142) and (143) are substituted into (146) then,

$$A_{12} = \tfrac{1}{2}B_1\left(x_2\frac{dy}{d\tau} - y_2\frac{dx}{d\tau}\right). \tag{148}$$

But the right-hand member of (148) is B_1 times the areal velocity* of the satellite, which by Kepler's Third Law is simply

$$A_{12} = \tfrac{1}{2}B_1k\sqrt{p} \tag{149}$$

where

$$\begin{aligned} p &= a(1 - e^2) \\ k &= \text{the Gaussian constant for earth satellites} \\ &= 0.07436574 \text{ min}^{-1}. \end{aligned}$$

Similar expressions exist for A_{23} which parallel (148) and (149) with subscript 3 substituting for 1. The area enclosed by r_1, r_3 and the connecting chord differs a bit from either A_{12} or A_{23} and is

$$\begin{aligned} A_{13} &= \tfrac{1}{2}(x_1y_3 - y_1x_3) \\ &= \tfrac{1}{2}(A_1B_3 - B_1A_3)k\sqrt{p}. \end{aligned} \tag{150}$$

Now by explicitly expressing the A_i, B_i factors of (144) and (145) in the sector area equations (149) (150), we have

$$A_{12} = \tfrac{1}{2}k\sqrt{p}\tau_3\left[1 - \frac{\tau_3^2}{6r_2^3} - \frac{\tau_3^3}{4r_2^4}\frac{dr}{d\tau} + \cdots\right] \tag{151}$$

$$A_{23} = \tfrac{1}{2}k\sqrt{p}\tau_1\left[1 - \frac{\tau_1^2}{6r_2^3} + \frac{\tau_1^3}{4r_2^4}\frac{dr}{d\tau} + \cdots\right] \tag{152}$$

$$A_{13} = \tfrac{1}{2}k\sqrt{p}\tau_2\left[1 - \frac{\tau_2^2}{6r_2^3} + \frac{\tau_2(\tau_1^2 - \tau_3)}{4r_2^4}\frac{dr}{d\tau} + \cdots\right]. \tag{153}$$

* See Ref. 14; Ref. 24, p. 5; and Ref. 9, p. 26.

The m_1 and m_3 equations follow directly from the above as

$$m_1 = \frac{A_{23}}{A_{13}} = \frac{\tau_1}{\tau_2}\left[1 + \frac{\tau_3(\tau_2 + \tau_1)}{6r_2^3} + \frac{\tau_3(\tau_3^2 + \tau_1\tau_3 - \tau_1^2)}{4r_2^4}\frac{dr}{d\tau} + \cdots\right] \tag{154}$$

$$m_3 = \frac{A_{12}}{A_{13}} = \frac{\tau_3}{\tau_2}\left[1 + \frac{\tau_1(\tau_2 + \tau_3)}{6r_2^3} - \frac{\tau_1(\tau_1^2 + \tau_1\tau_3 - \tau_3^2)}{4r_2^4}\frac{dr}{d\tau} + \cdots\right]. \tag{155}$$

REFERENCES

1. Spitzer, L., Perturbation of a Satellite's Orbit, J. Brit. Interplanetary Soc., *9*, 1950, p. 131.
2. Corneir, L. N., Goodwin, W., and Squires, R. K., Simplified Satellite Predictions from Modified Orbital Elements, IGY Satellite Report Series, No. 7, Natl. Acad. Sci., Natl. Res. Council, Washington, D.C., 1959.
3. Ossanna, J. F., Jr., The Generation of Look Angles from Regularly Available Mean Orbital Elements for 1960 Iota One, Photographic Science and Engr., Nov.–Dec., 1962, pp. 342–350.
4. Moulton, F. R., *An Introduction to Celestial Mechanics*, 2nd rev. ed., The MacMillan Co., New York, 1923.
5. *The American Ephemeris and Nautical Almanac for 1962*, U.S. Govt. Printing Office, 1960.
6. de LaPlace, Marquis, *Mécanique Céleste*, tr. Bowditch, N., Hilliard, Gray, Little and Wilkins, Boston, 1829.
7. Gauss, K. F., *Theoria Motus Corporum Coelestium in Sectionibus Conicus Solum Ambientum*, Hamburg, 1809.
8. Danby, J. M. A., *Fundamentals of Celestial Mechanics*, The MacMillan Co., New York, 1962.
9. Herget, Paul, *The Computation of Orbits*, publ. by author, 1948.
10. Smart, W. M., Celestial Mecbanics, London, Longmans, Green, 1953, Ch. 5.
11. Claus, A. J., Blackman, R. B., Halline, E. G., and Ridgeway, W. C., III, Orbit Determination and Prediction, and Computer Programs, B.S.T.J., *42*, July, 1963, part 2.
12. Notes of the Summer Institute on Dynamical Astronomy at Yale University, July 1959, Yale University Observatory, New Haven, Conn., 1960, pp. 97–100.
13. Blanco, V. M., and McCuskey, S. W., *Basic Physics of the Solar System*, Addison-Wesley Publishing Co., Reading, Mass, 1961.
14. Smart, W. M., *Textbook on Spherical Astronomy*, Cambridge University Press, 1956.
15. *The Explanatory Supplement to the American Ephemeris and Nautical Almanac*, Her Majesty's Stationery Office, London, 1961.
16. King-Hele, D. G., The Earth's Gravitational Potential, in *The Earth Today*, ed. Crook, A. H., and Gaskell, T. F., Royal Astronomical Soc., Interscience Publ., New York.
17. O'Keefe, J. A., Eckels, A., and Squires, R. K., The Gravitational Field of the Earth, Astrophys. J., *64*, Sept., 1959.
18. Allen, C. W., *Astrophysical Quantities*, Athlone Press, 1955.
19. Jeffreys, H., *The Earth*, Cambridge University Press, 1952.
20. Lecar, M., Sorenson, J., and Eckels, A., J. Geophys. Res., *64*, 1959, pp. 209–216.

21. Merson, R. H., The Motion of a Satellite in an Axisymmetrical Gravitational Field, in *The Earth Today*, ed. Crook, A. H., and Gaskell, T. F., Royal Astronomical Soc., Interscience Publ., New York.
22. Proc. Ninth National Communications Symposium, Oct., 1963, Western Periodicals Co., pp. 146–155.
23. *Handbook of Chemistry and Physics*, 28th ed., Chemical Rubber Publishing Co., Cleveland, O., 1944.
24. McCuskey, S. W., *Introduction to Celestial Mechanics*, Addison-Wesley Publishing Co., Reading, Mass.